

# Introduction to Powder Diffraction



**Joel Reid,  
Industrial Scientist,  
Canadian Light  
Source**

**Monday,  
October 26, 2020**



Canadian Light Source   Centre canadien de rayonnement synchrotron

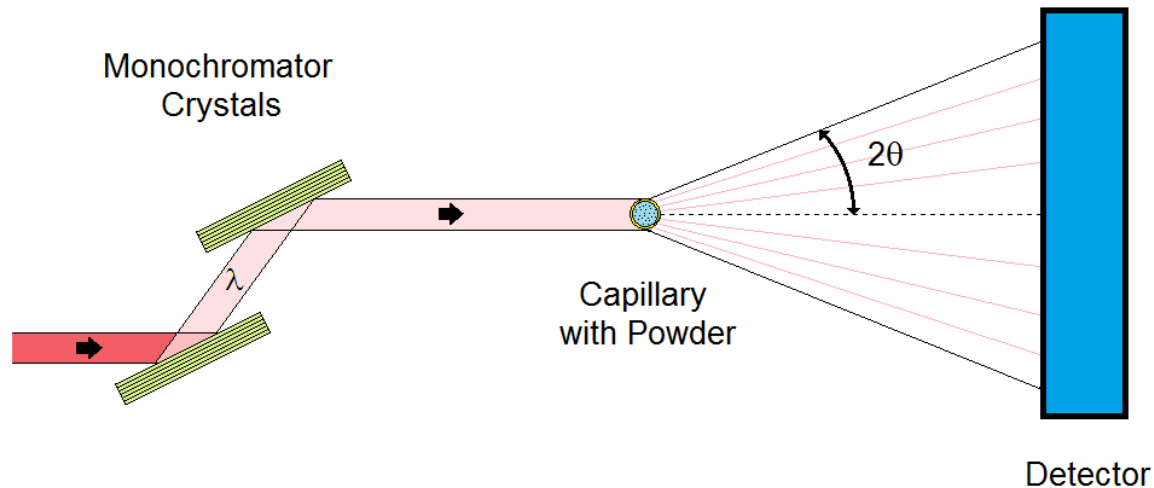
THE BRIGHTEST LIGHT IN CANADA | [lightsource.ca](http://lightsource.ca)

# Outline

1. A brief history of powder diffraction and the Rietveld method.
2. An introduction to powder diffraction and Rietveld refinement with applications and examples.
3. Examination of the main factors affecting Bragg reflection positions and intensities in powder diffraction patterns.

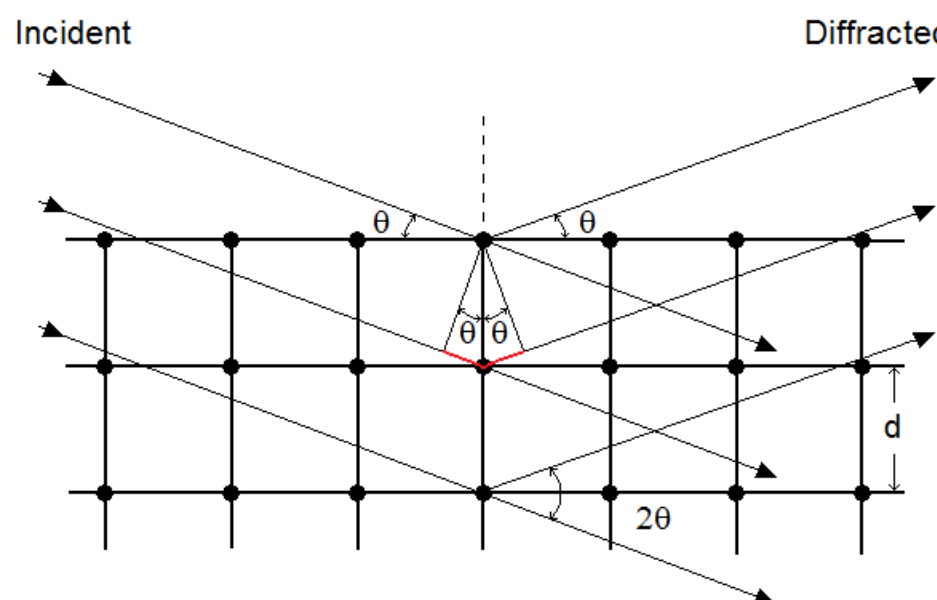


# What is Powder Diffraction?

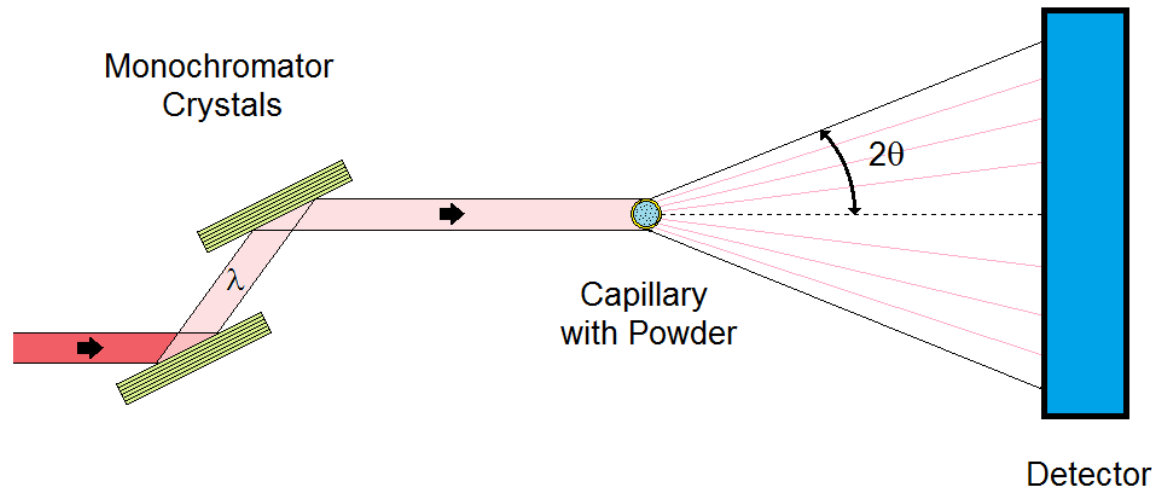


**Bragg's Law**

$$\lambda = 2d_{hkl} \sin \theta$$

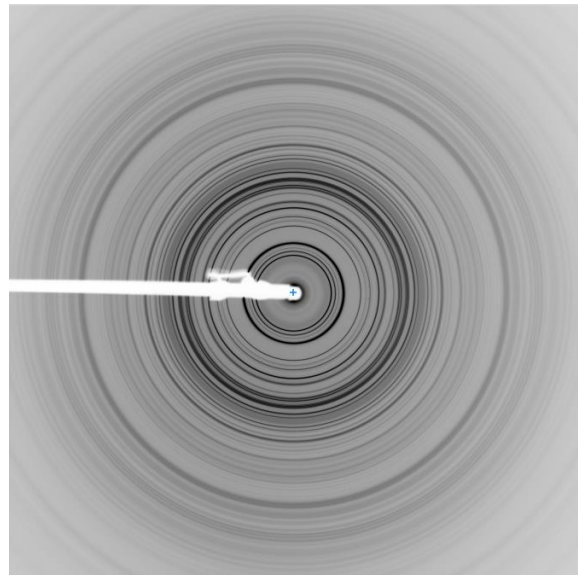


# What is Powder Diffraction?

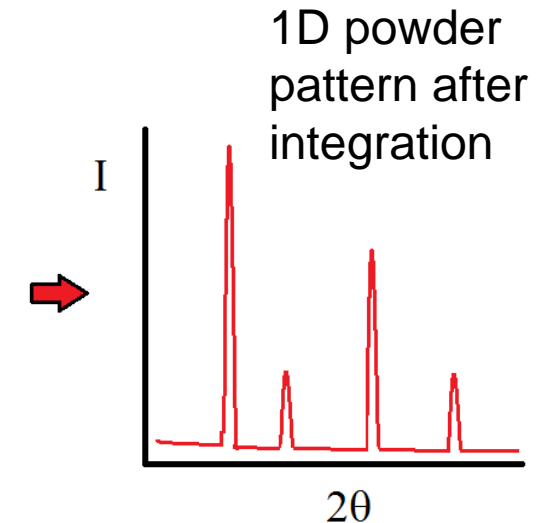
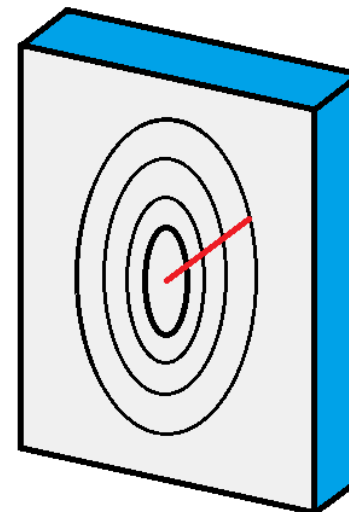


**Bragg's Law**

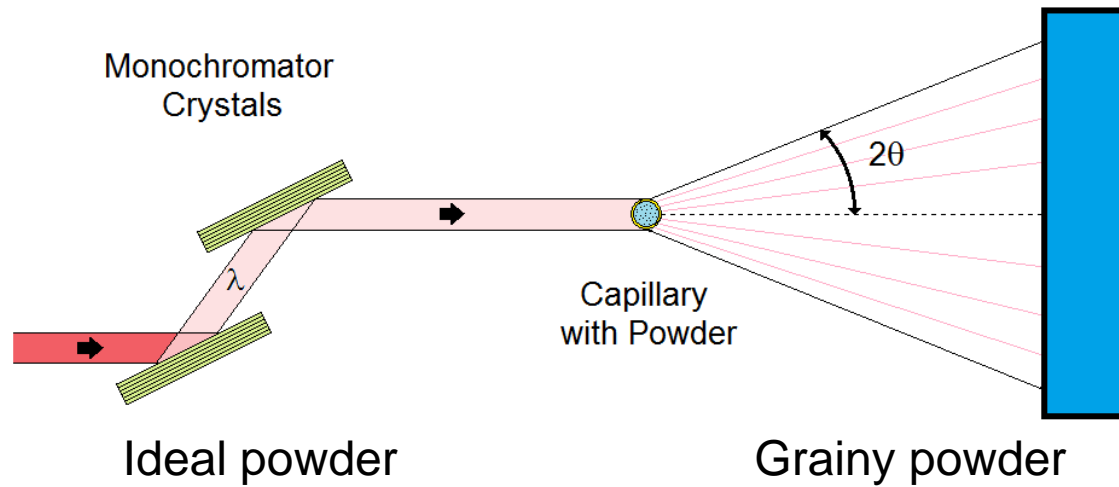
$$\lambda = 2d_{hkl} \sin \theta$$



2D powder ring pattern on detector

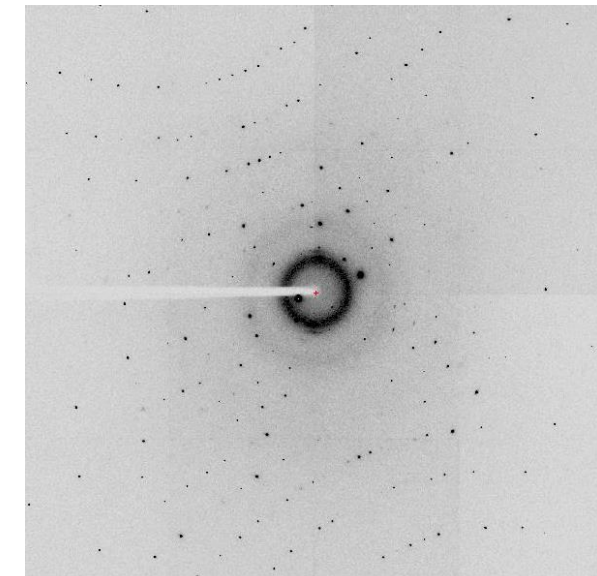
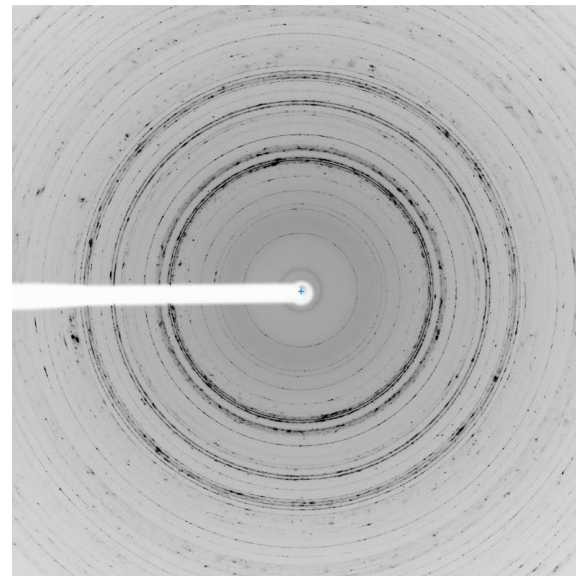
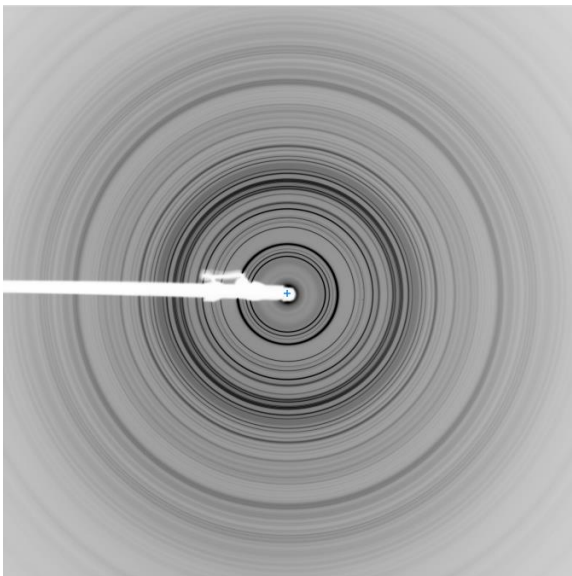


# What is Powder Diffraction?



**Bragg's Law**

$$\lambda = 2d_{hkl} \sin \theta$$



Single crystal pattern  
courtesy of Denis Spasyuk.



Canadian  
Light  
Source

Centre canadien  
de rayonnement  
synchrotron

# What is Powder Diffraction?

- Powder diffraction is a flexible technique for studying crystalline materials with crystal sizes ranging from microns to nanometers, with high information content.
- Powder diffraction can be used to:
  - Identify different crystalline phases in a mixture.
  - Quantify the proportions of different crystalline phases in a mixture, including the amorphous content.
  - Solve and refine the crystal structure of unknown or new crystalline phases.
  - Quantify microstructural features of crystalline materials like strain and the size (shape) of the crystallites.
  - Examine local structure of disordered, poorly crystalline and amorphous materials with Pair Distribution Function (PDF) analysis.



# A Brief History of Powder Diffraction

- **1895:** X-rays are first discovered by Wilhelm Röntgen.
- **1912:** Max von Laue demonstrates diffraction of X-rays by crystals.
- **1913:** The Bragg's demonstrate the solution of crystal structures with diffraction.
- **1916:** The first diffraction cameras are independently devised by Debye & Scherrer (Switzerland) and Hull (U.S.).
- **1935:** The first powder diffractometer is designed and built by LeGalley.
- **1941:** The Joint Committee for Chemical Analysis by Powder Diffraction Methods (the initial precursor to the ICDD) was founded in 1941 and subsequently created the Powder Diffraction File™ for phase identification.
- **1947:** The first commercial powder diffractometer is introduced by Phillips.



# A Brief History of Powder Diffraction (cont.)

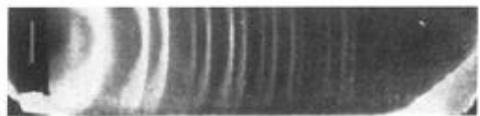


FIG. 8. Silicon.

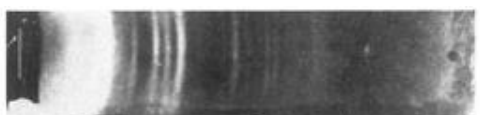


FIG. 10. Magnesium.



FIG. 11. Graphite.

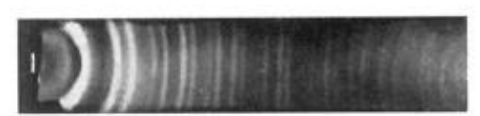


FIG. 12. Diamond.

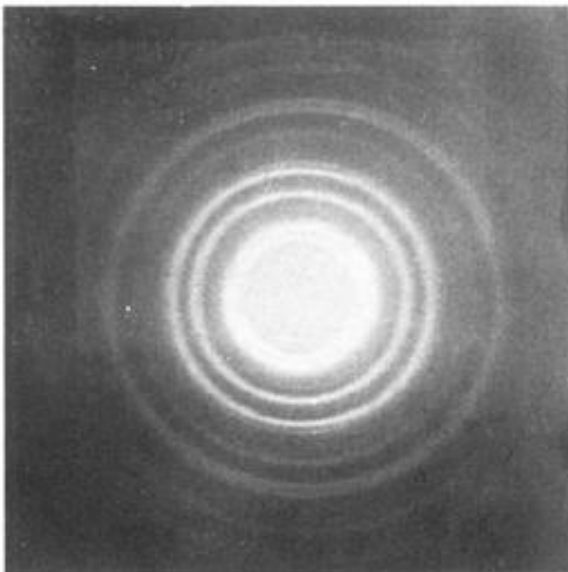
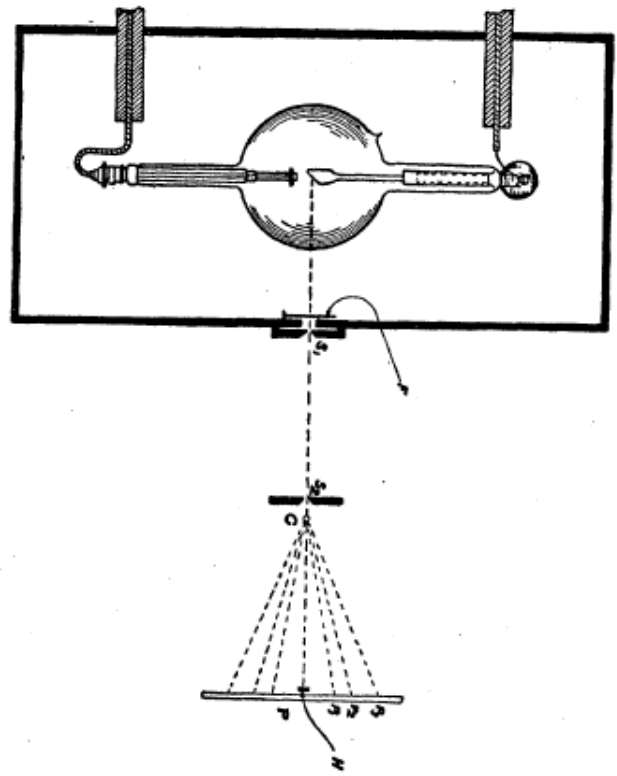


FIG. 1. Aluminium.



- The powder camera designed by Albert Hull, and some of his initial powder diffraction patterns.

Hull, A. W. Phys. Rev. 10 (1917) 661-696



# A Brief History of Powder Diffraction (cont.)

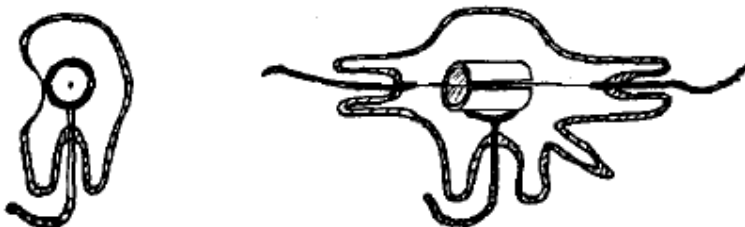


FIG. 1. Diagram of Geiger-Müller counter.

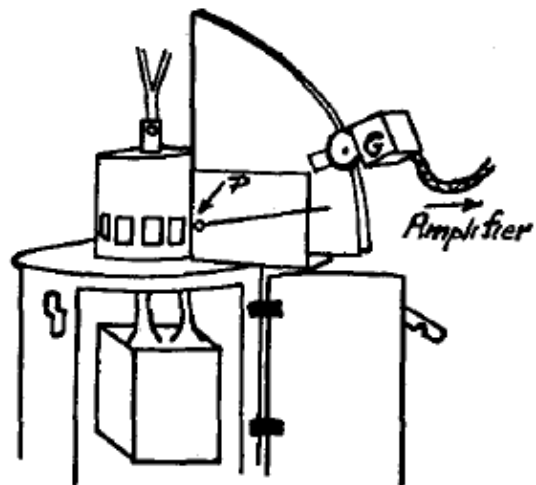


FIG. 3. Diagram of x-ray apparatus.

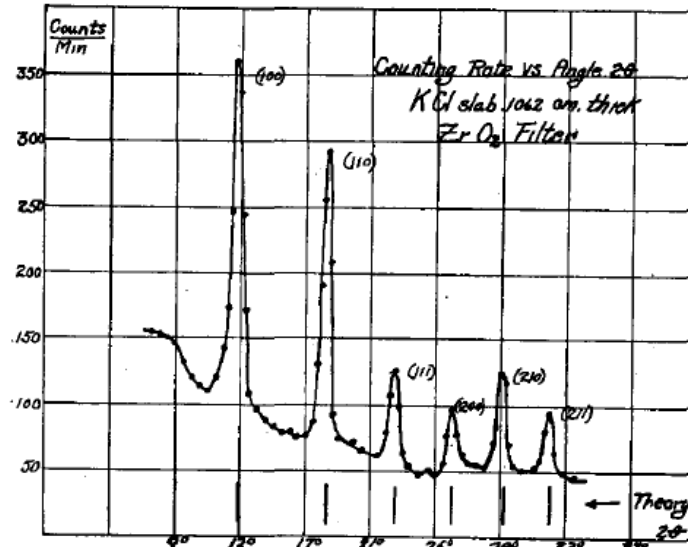


FIG. 5. Diffraction pattern of KCl.

- The first powder diffractometer, designed by Donald LeGalley, based on a Geiger–Müller tube detector.



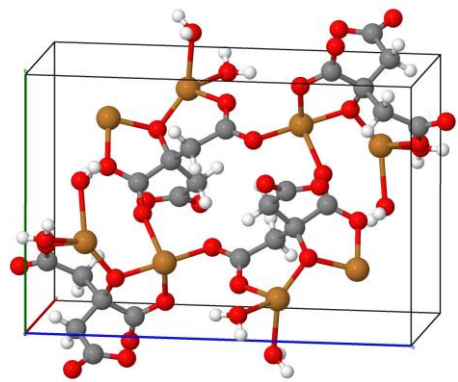
# A Brief History of Powder Diffraction (cont.)

- **1966-1969:** Hugo Rietveld and colleagues develop the whole pattern refinement approach (the Rietveld Method) using neutron powder diffraction data.
- **1977-1978:** A number of scientists (including Young, von Dreele, Cox, Malmros, Thomas and Glazer, among others) begin using the Rietveld method with laboratory and synchrotron X-ray powder diffraction data.
- **1986-1988:** The widely used Rietveld programs GSAS (Larson & von Dreele) and FullProf (Rodriguez-Carvajal) are first developed. Rietveld refinement with neutron powder diffraction data proves indispensable in the determination of the structure of the high temperature superconductor,  $\text{YBa}_2\text{Cu}_3\text{O}_{7-x}$ , and subsequent superconducting materials.
- **1980's to present:** Powder diffraction and Rietveld refinement have seen a consistent increase in usage with constantly improving diffractometer technology, software capabilities, theoretical understanding, and significantly expanded access to synchrotron and neutron facilities. Structure solution and PDF analysis from powder diffraction data is increasingly routine.

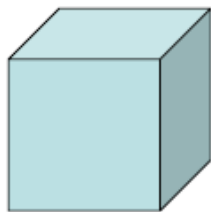


# The Problem of Peak Overlap

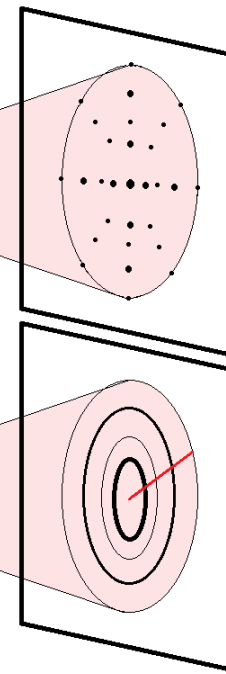
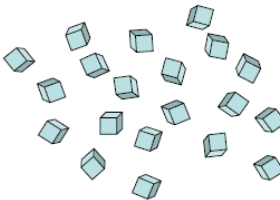
3D crystal structure



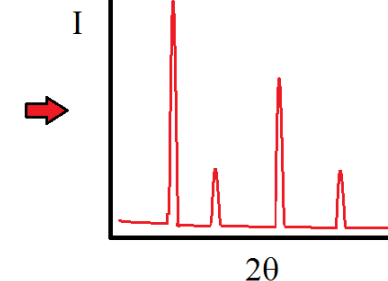
Single Crystal



Powder



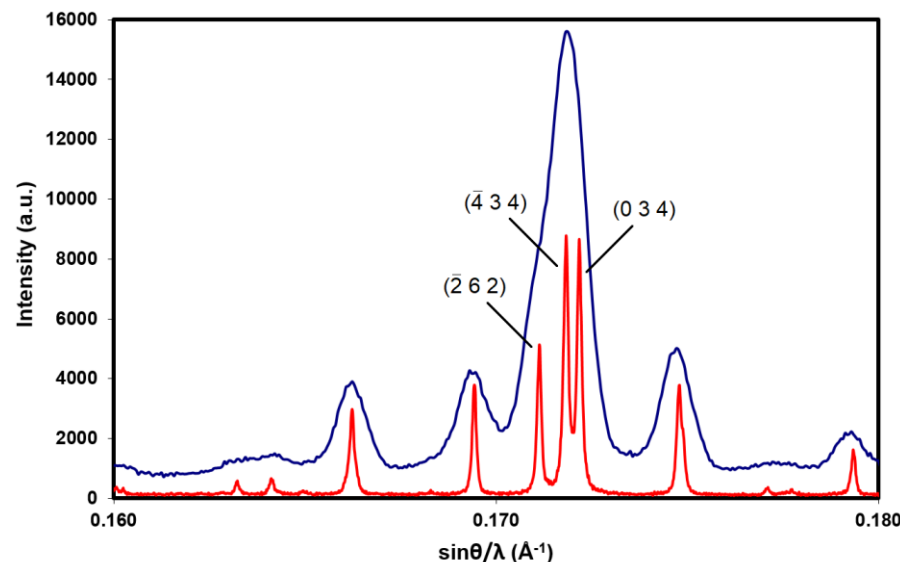
1D powder pattern



- Powder diffraction suffers an inherent loss of information, due to the compression of 3D crystalline structure information into 1D.
- For all but the simplest, high symmetry compounds, peak overlap becomes an issue for determining the intensities of individual reflections.

# The Problem of Peak Overlap (cont.)

- Before the Rietveld method (1950's and 60's), powder diffraction was most commonly used for qualitative fingerprinting of compounds and mixtures, rather than more quantitative work.
- Quantitative methods tended to use small numbers of isolated peaks to overcome the problem of peak overlap. Inventive, but ultimately limited, methods were developed to estimate intensities for overlapping peaks.
- Actual structure solution from powder data was exceedingly rare, and focused mainly on high symmetry compounds with well resolved peaks.



# The Rietveld Method

- Development of full pattern fitting required (1) sufficient knowledge of diffraction physics and (2) the advent of powerful digital computers.
- Hugo Rietveld (with colleagues at Petten) was the first person to develop (and widely share) computer code for full powder pattern refinement, using data obtained from neutron diffraction:

*J. Appl. Cryst.* (1969). 2, 65

## A Profile Refinement Method for Nuclear and Magnetic Structures

By H. M. RIETVELD

*Reactor Centrum Nederland, Petten (N.H.), The Netherlands*

(Received 29 November 1968)

A structure refinement method is described which does not use integrated neutron powder intensities, single or overlapping, but employs directly the profile intensities obtained from step-scanning measurements of the powder diagram. Nuclear as well as magnetic structures can be refined, the latter only when their magnetic unit cell is equal to, or a multiple of, the nuclear cell. The least-squares refinement procedure allows, with a simple code, the introduction of linear or quadratic constraints between the parameters.

Rietveld, H.M. *Acta Cryst.* 22 (1967) 151-152.

Rietveld, H.M. *J. Appl. Cryst.* 2 (1969) 65-71.

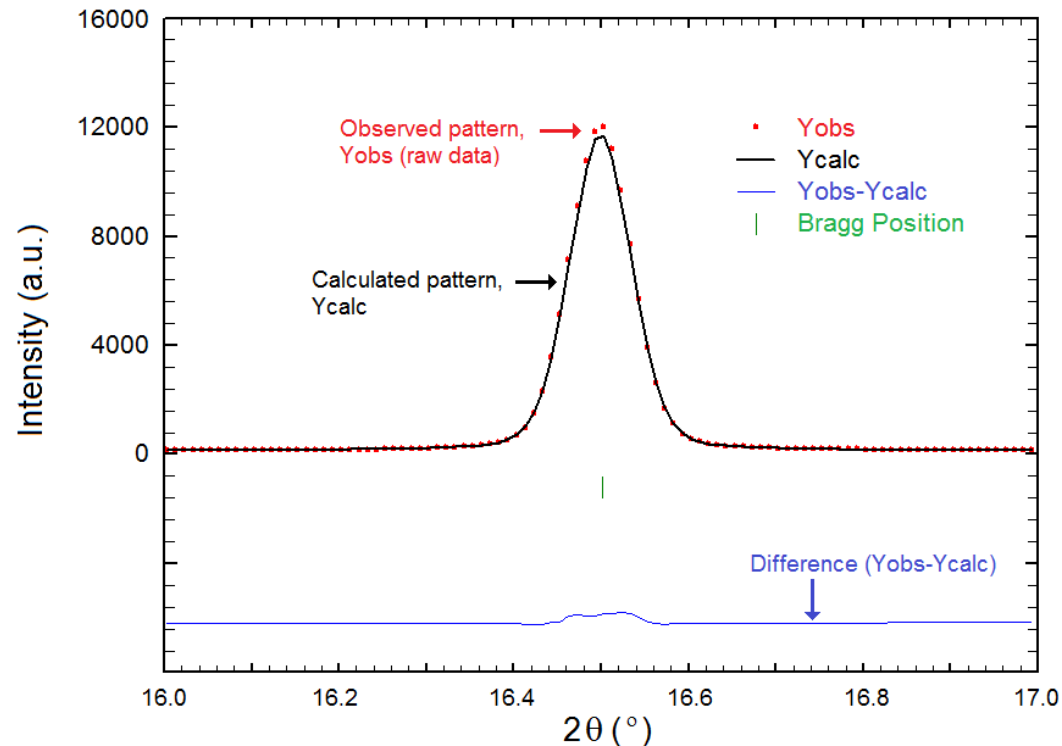
van Laar, B. & Schenk, H. *Acta Cryst.* A74 (2018) 88-92.



# What is the Rietveld Method?

- The Rietveld method is a **least squares refinement** technique used to refine the full powder diffraction pattern.
- The observed data is modeled using a structural model for the phase(s) present, and the difference between the observed ( $Y_o$ ) and calculated ( $Y_c$ ) patterns is minimized during refinement:

$$M = \sum w(Y_o - Y_c)^2$$



Rietveld, H.M. Acta Cryst. 22 (1967) 151-152.

Rietveld, H.M. J. Appl. Cryst. 2 (1969) 65-71.

Young, R.A., ed. The Rietveld Method. Oxford: New York, 1993.



# Powder Diffraction Pattern Content

- Powder diffraction patterns contain a lot of information!

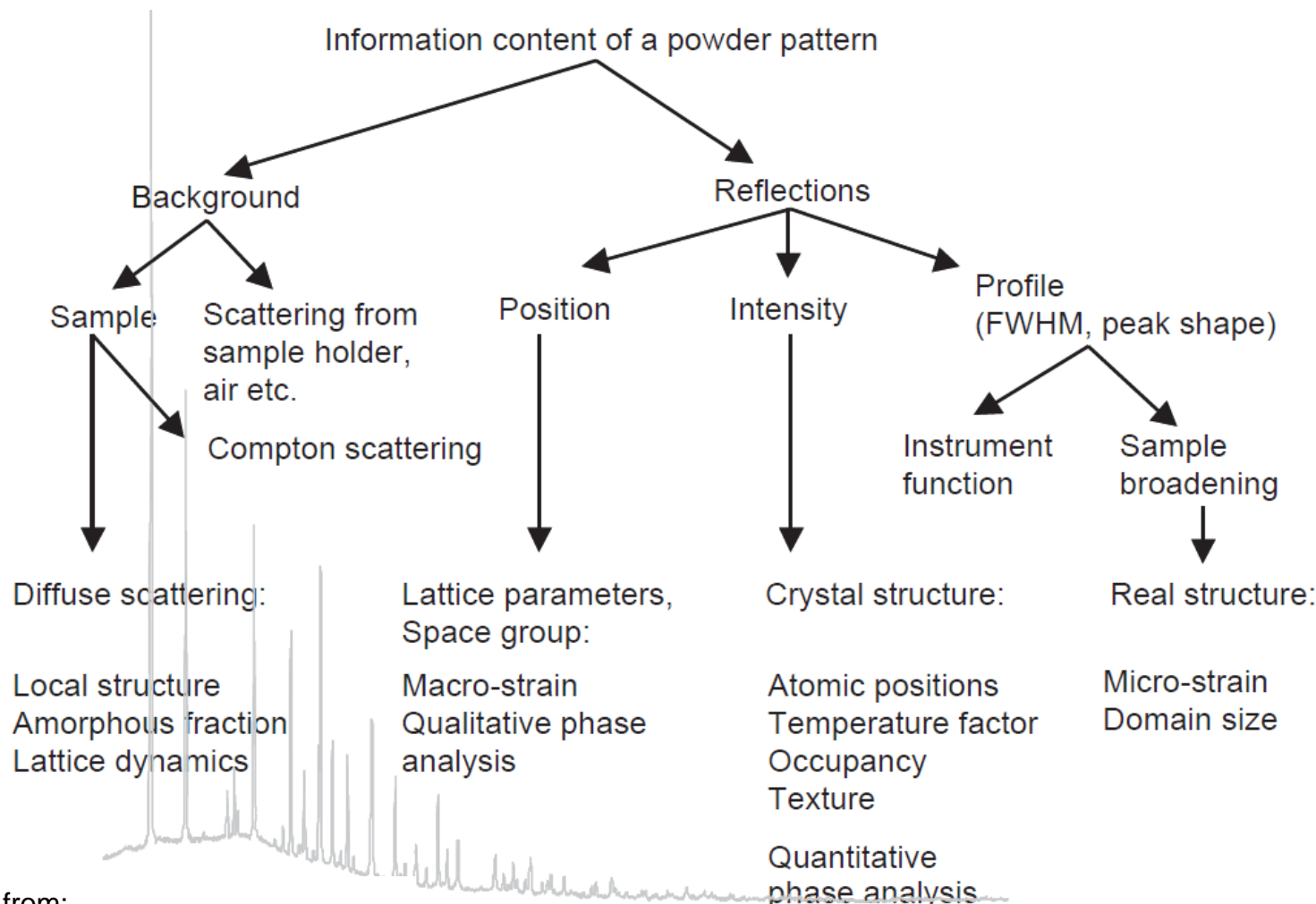


Figure taken from:

Powder Diffraction, Theory and Practice.

Edited by R.E. Dinnebier & S.J.L. Billinge.

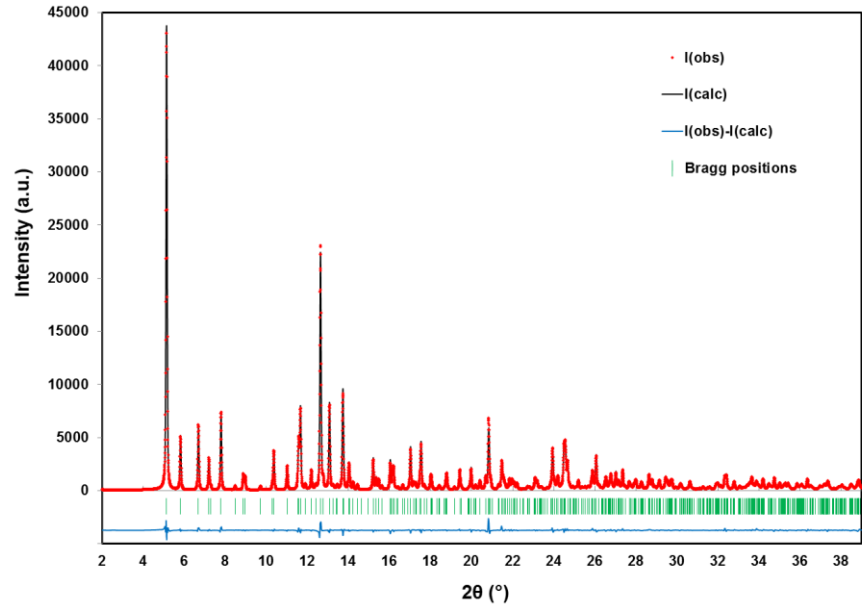
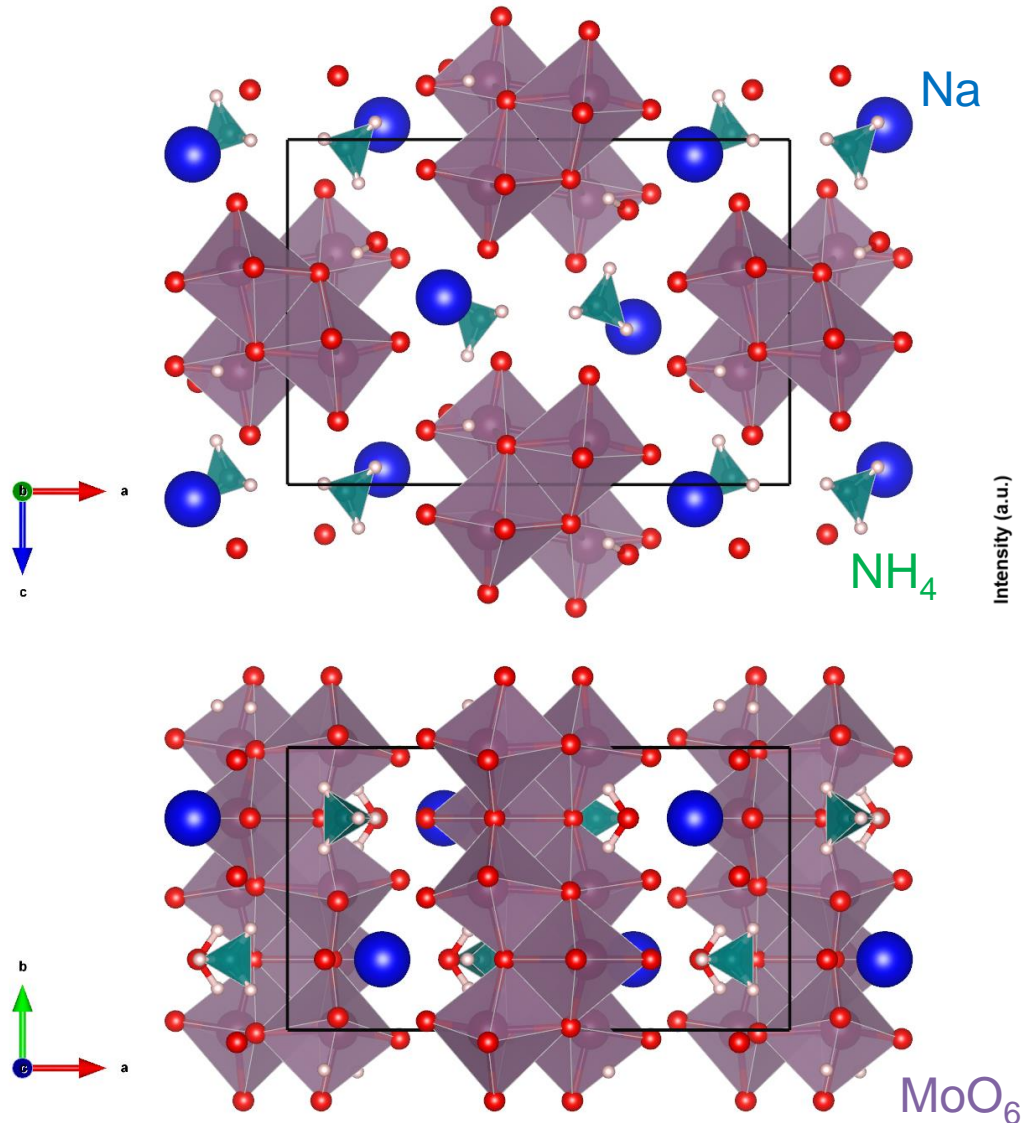
(RSC Publishing: Cambridge, 2008)

# Rietveld Method Applications

- What can we analyze with the Rietveld method?
  - Crystal structure:
    - Lattice parameters, atomic positions, thermal displacement parameters, site occupancies.
  - Phase Composition:
    - Quantitative phase analysis of mixtures of crystalline phases.
    - Estimation of amorphous content with an internal standard.
  - Microstructure:
    - Texture/preferred orientation, crystallite size and strain.
- Most of these properties can be studied as functions of time, temperature, pressure or other variables to understand the *in situ* or *in operando* behavior of materials.



# Applications: Structure Solution & Refinement



Reid, J.W., Kaduk, J.A. & Olson, J.A.  
Powder Diffraction 32 (2017) 140-147.



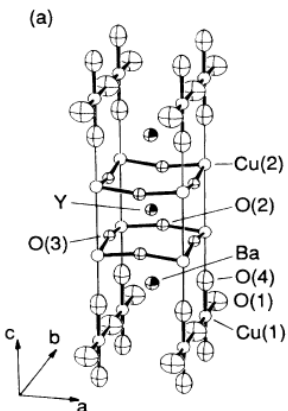
Canadian  
Light  
Source

Centre canadien  
de rayonnement  
synchrotron

THE BRIGHTEST LIGHT IN CANADA | [lightsource.ca](http://lightsource.ca)

# Example: Structure of $\text{YBa}_2\text{Cu}_3\text{O}_{7-x}$ (YBCO)

Orthorhombic



Tetragonal

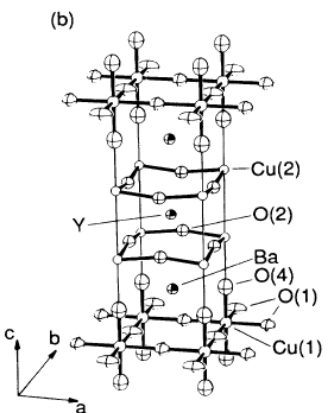
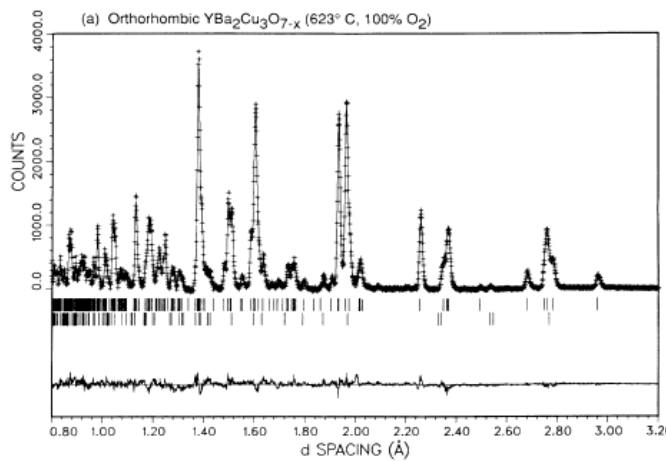


FIG. 2. Structure of  $\text{YBa}_2\text{Cu}_3\text{O}_{7-x}$ . (a) The orthorhombic  $Pmmm$  phase. (b) The tetragonal  $P4/mmm$  phase. Note that in the tetragonal phase the oxygen atoms are disordered in the  $z = 0$  plane.

- Neutron powder diffraction and Rietveld refinement were critical in the determination of the correct crystal structures of YBCO, the first high temperature superconductor.
- Single crystal methods gave different and incorrect structures due to crystal twinning.

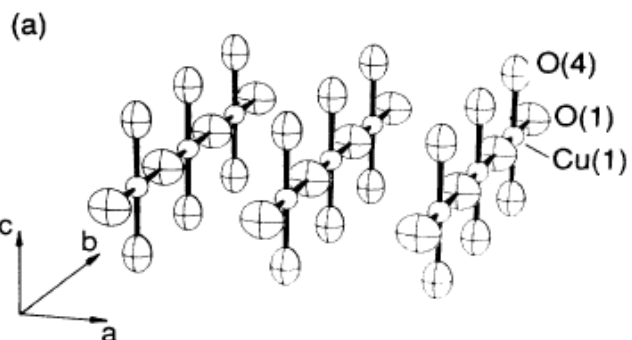


Jorgensen, J.D. et. al. Phys. Rev. B 36 (1987) 3608-3616.



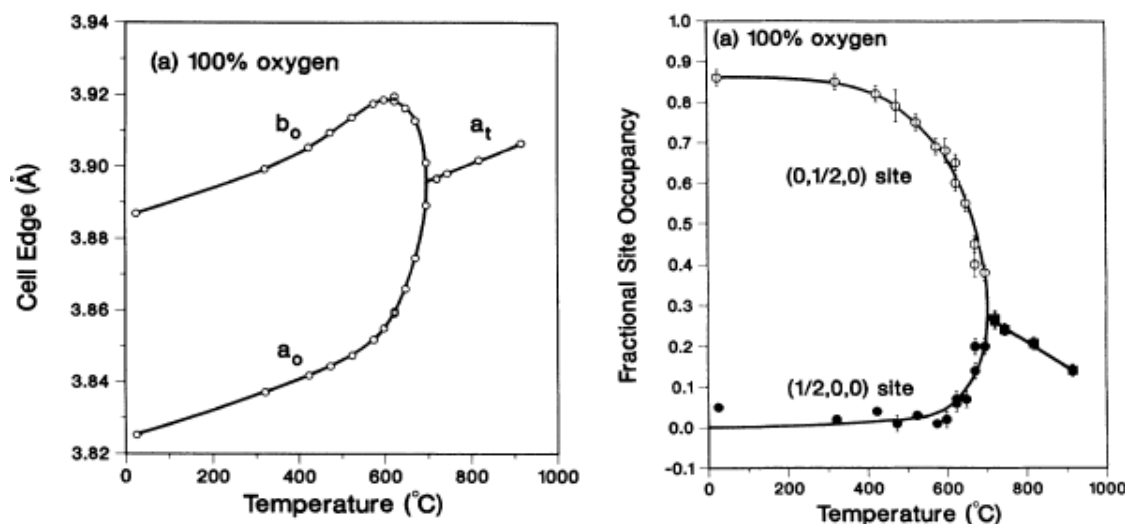
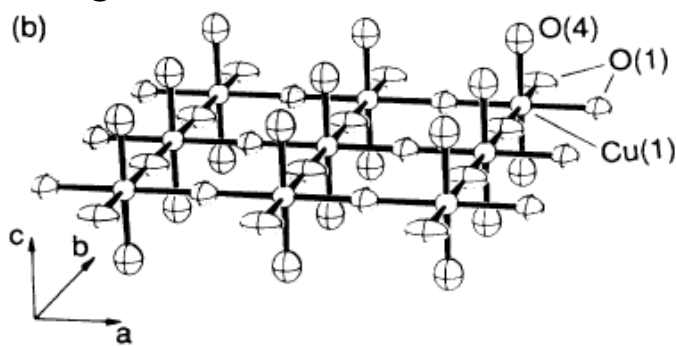
# Example: Structure of $\text{YBa}_2\text{Cu}_3\text{O}_{7-x}$ (YBCO)

Orthorhombic



- Oxygen ordering in the low temperature orthorhombic phase creates Cu-O 1-dimensional chains, which are important for superconductivity. Neutrons were critical for determining the oxygen positions and occupancies.

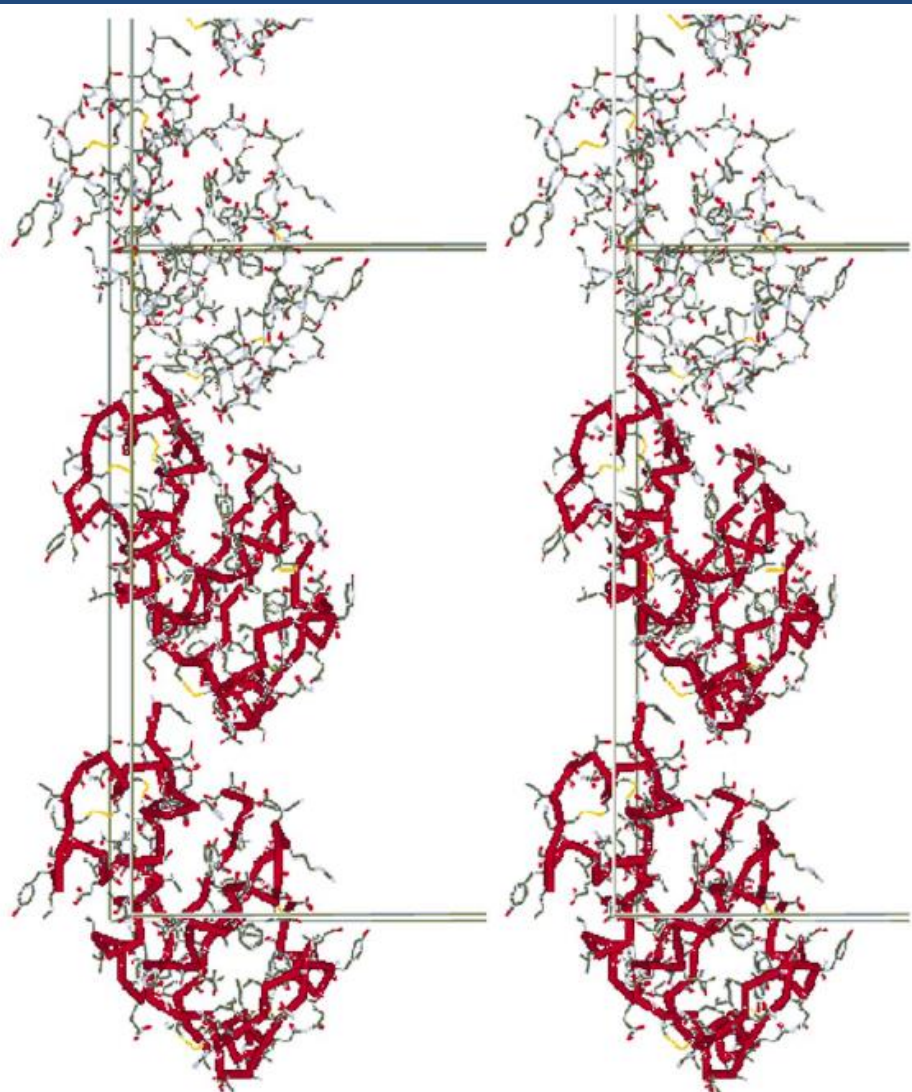
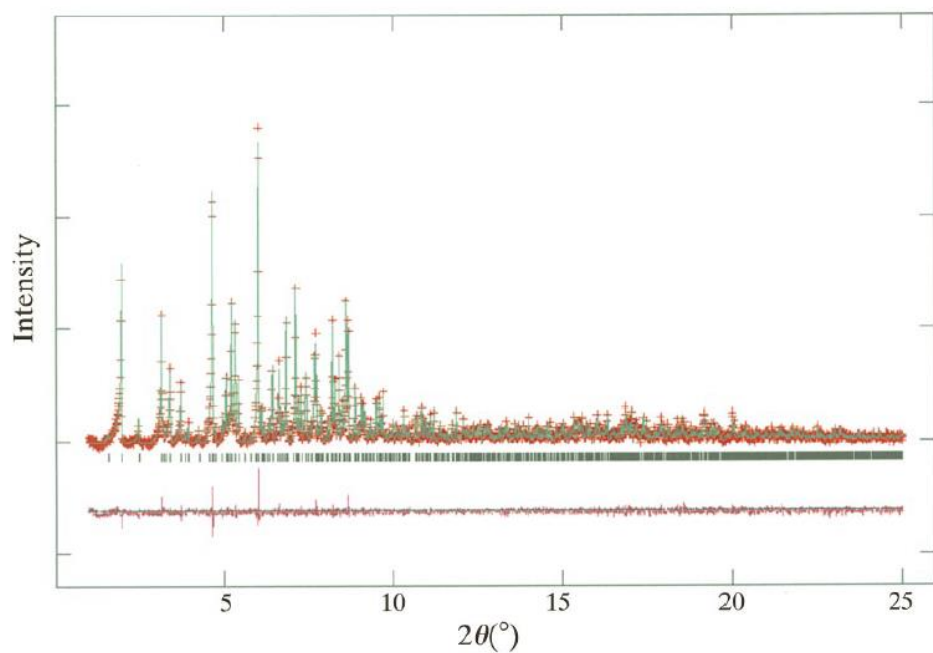
Tetragonal



Jorgensen, J.D. et. al. Phys. Rev. B 36 (1987) 3608-3616.



# Example: Solving Protein Structures



$T_3R_3$  human insulin Zn complex  
Space Group: R3  
 $a = 81.2780(7) \text{ \AA}$ ,  $c = 73.0389(9) \text{ \AA}$   
 $V = 417,860(8) \text{ \AA}^3$  (!)  
1630 atoms (!!)

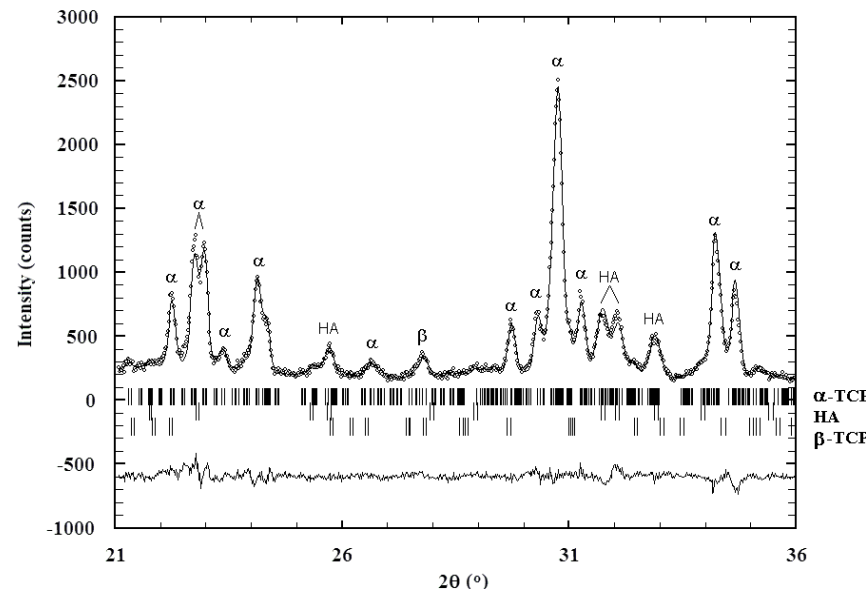
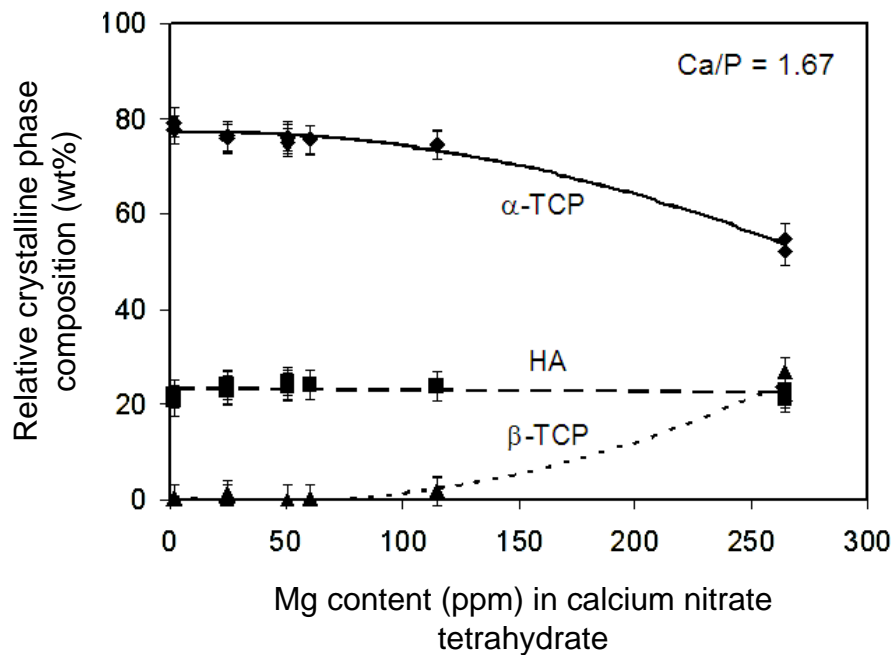
Von Dreele, R.B. et. al. *Acta Cryst. D56* (2000) 1549-1553.



# Applications: Phase Quantification

TCP → tricalcium phosphate,  $\text{Ca}_3(\text{PO}_4)_2$   
HA → calcium hydroxyapatite,  $\text{Ca}_5(\text{PO}_4)_3\text{OH}$

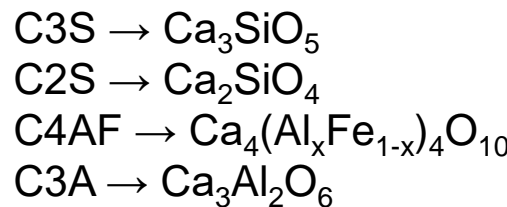
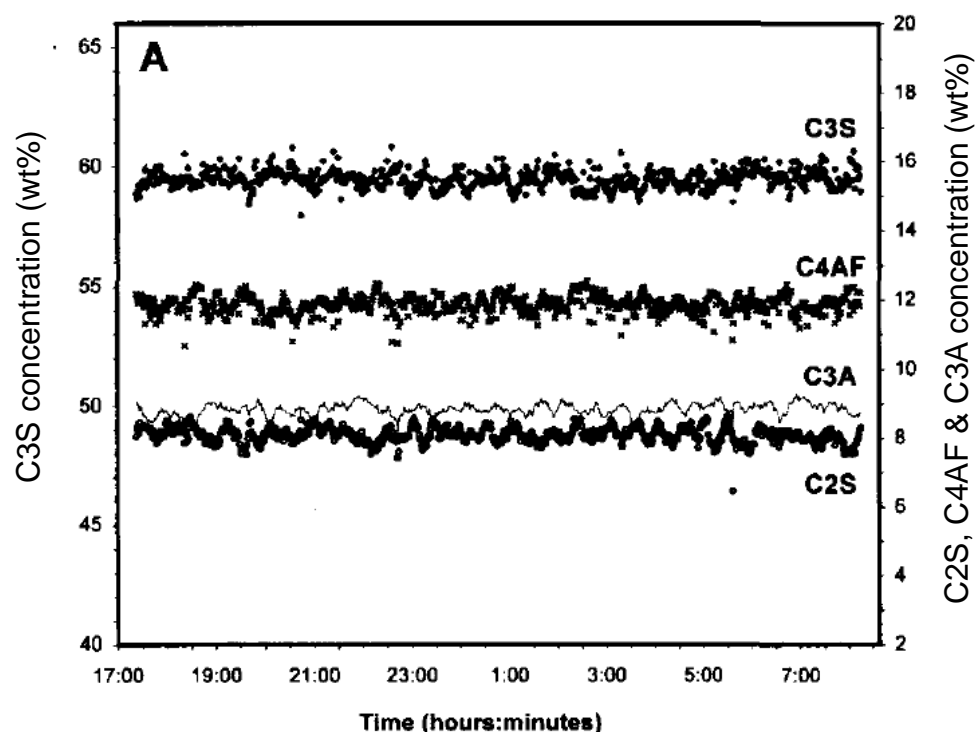
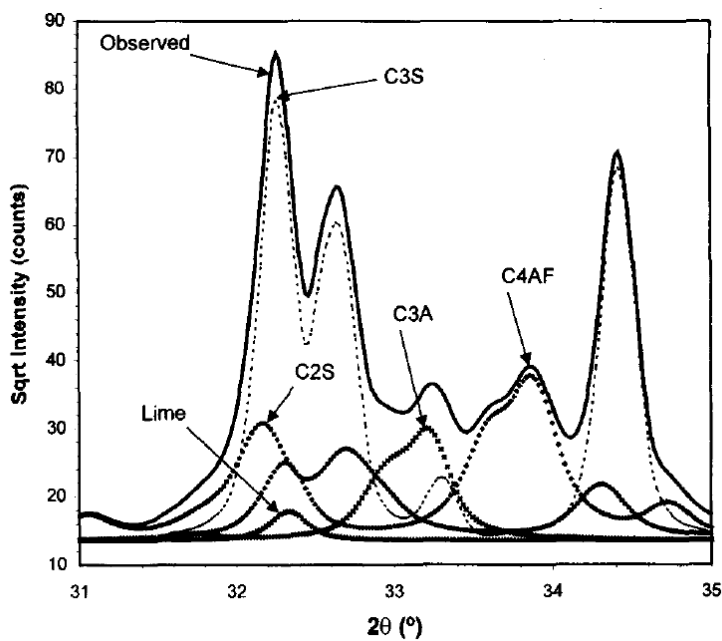
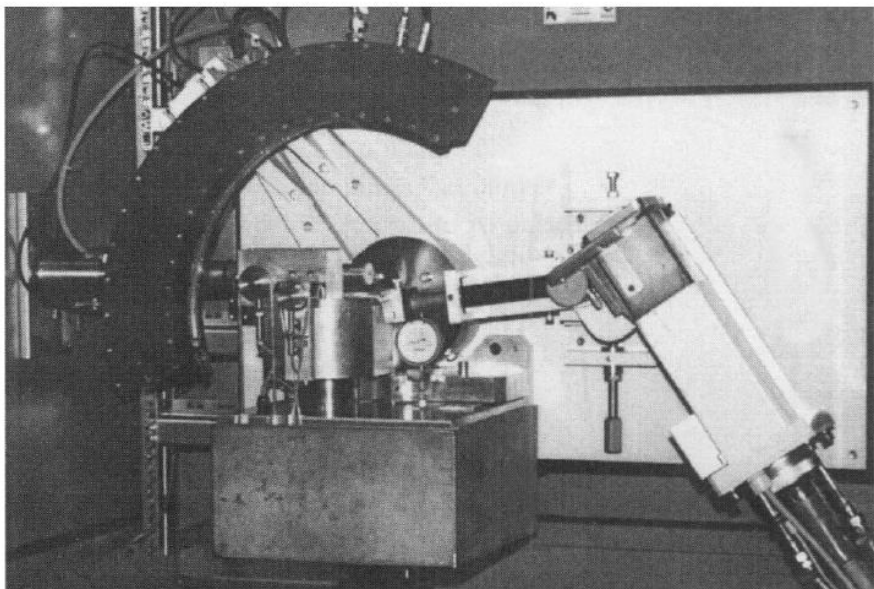
Reid, J.W. et. al. Mater. Lett. 61 (2007) 3851-3854.



- The influences of small chemistry changes (for instance, impurity concentration in a reactant) can significantly influence the phase composition of the end product.



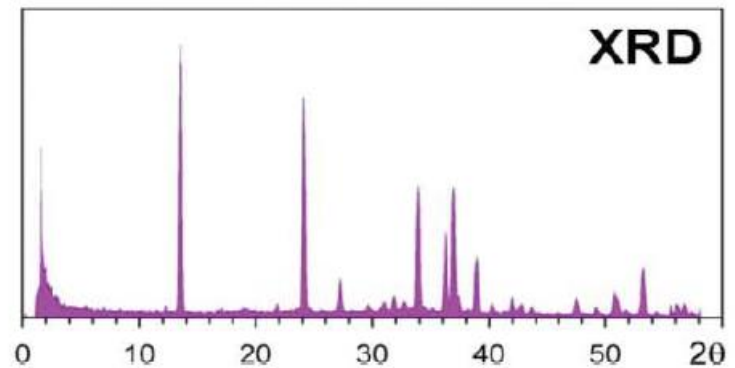
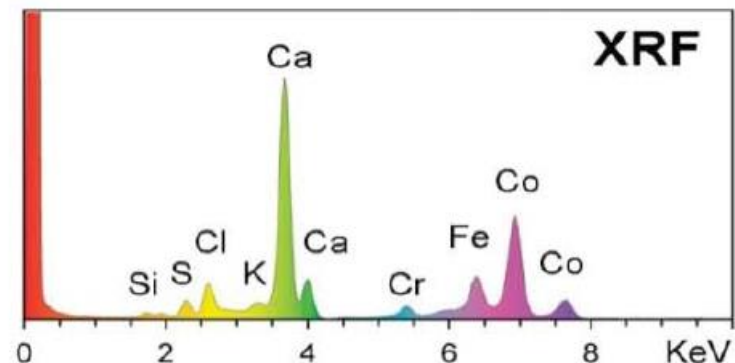
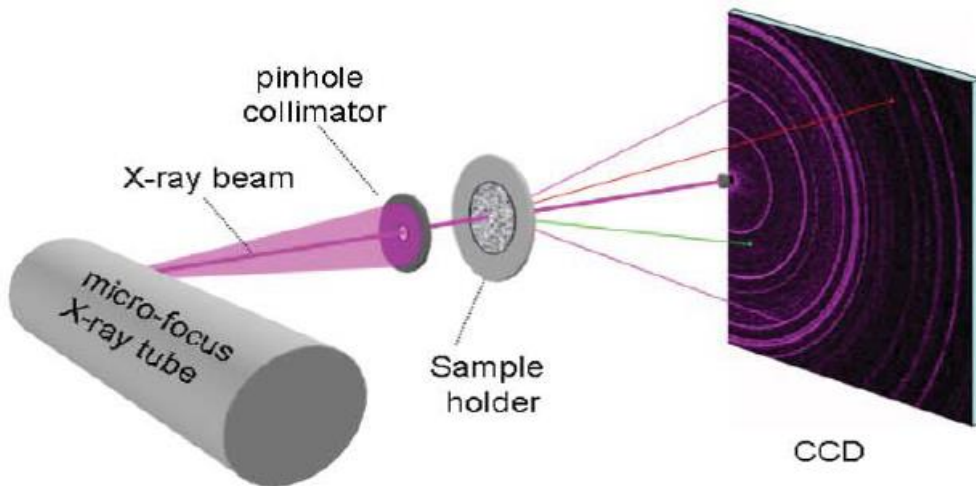
# Example: On-line QA/QC of Cement



Scarlett, N. V. Y. et. al. Powder Diffraction 16 (2001) 71-80.

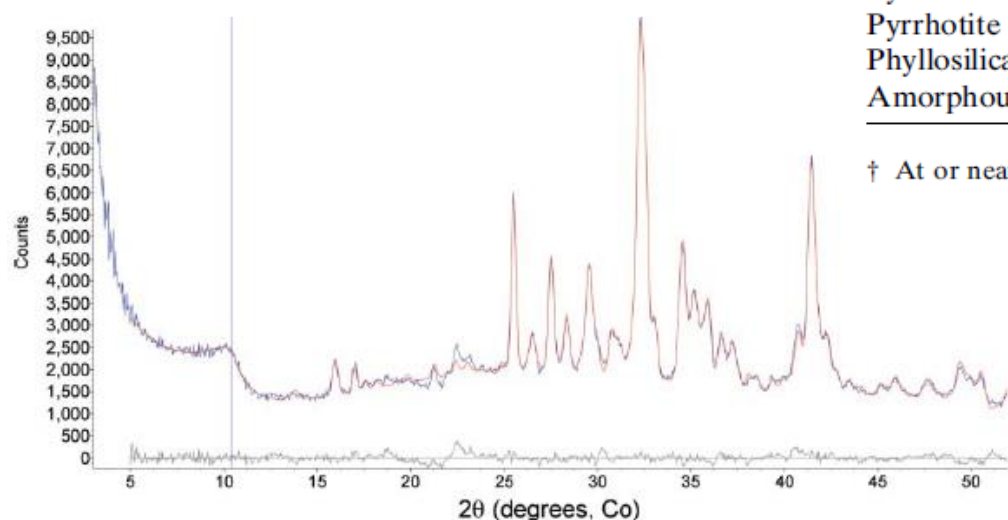
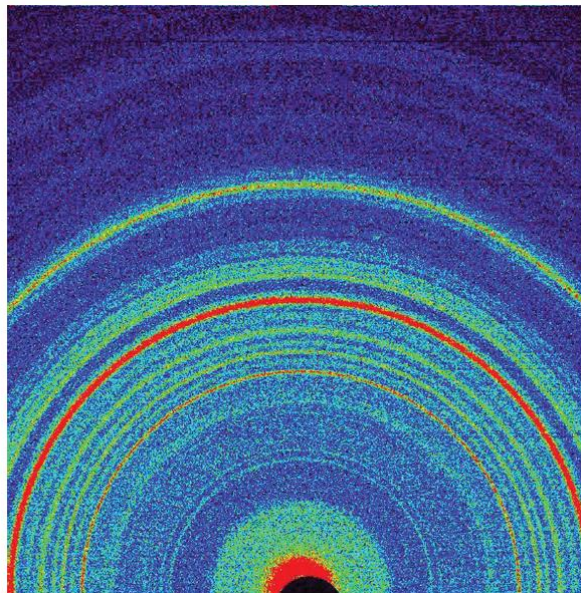
# Example: Rietveld QPA on Mars

- The CheMin XRD/XRF, one of ten analytical instruments on the Curiosity rover, which landed in the Gale crater in August 2012.



Bish, D.L. et. al. IUCrJ 1 (2014) 514-522.

# Example: Rietveld QPA on Mars



Mineral	John Klein	Cumberland
Plagioclase	22	22
Fe-forsterite	3	1
Augite	4	4
Pigeonite	6	8
Orthopyroxene	3	4
Magnetite	4	4
Anhydrite	3	1
Bassanite	1	1
Sanidine	1	2
Quartz	0.4†	0.1†
Hematite	0.6†	1
Ilmenite		0.5†
Akaganeite	1	2
Pyrite	0.3†	
Pyrrhotite	1	1
Phyllosilicate	22	18
Amorphous	28	31

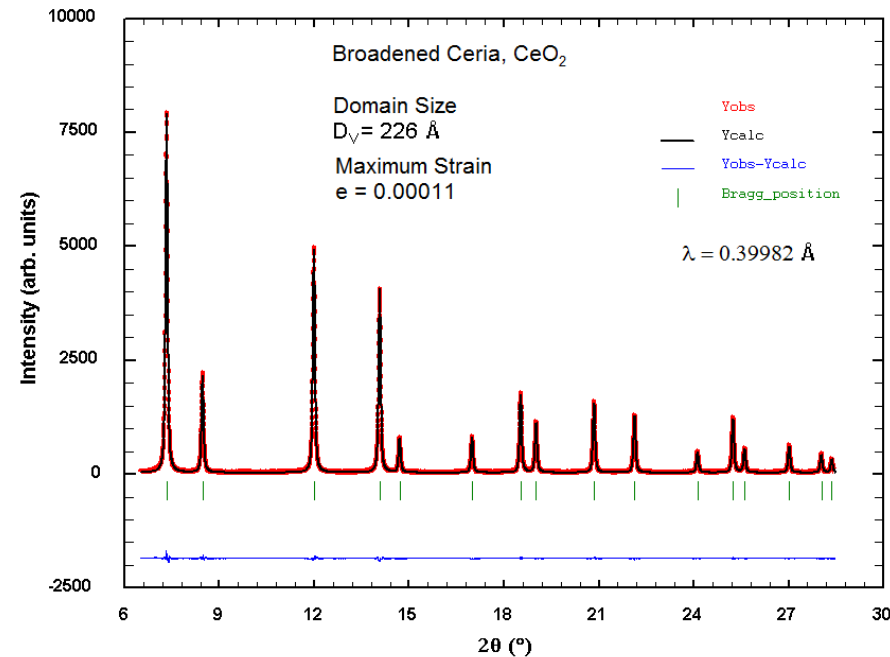
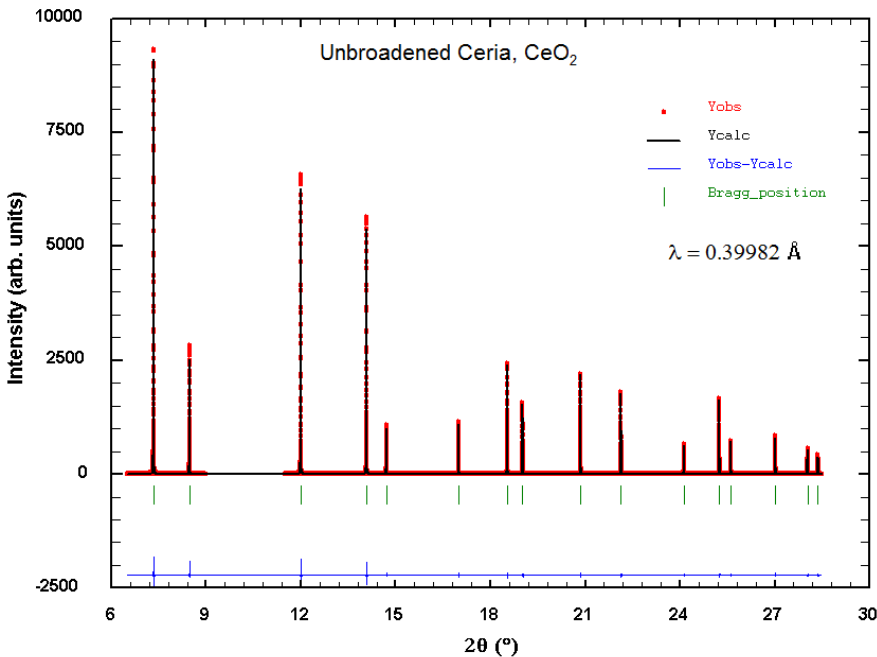
† At or near the detection limit.

Mudstone compositions from two locations on Mars.

Bish, D.L. et. al. IUCrJ 1 (2014) 514-522.



# Applications: Crystallite Size and Strain

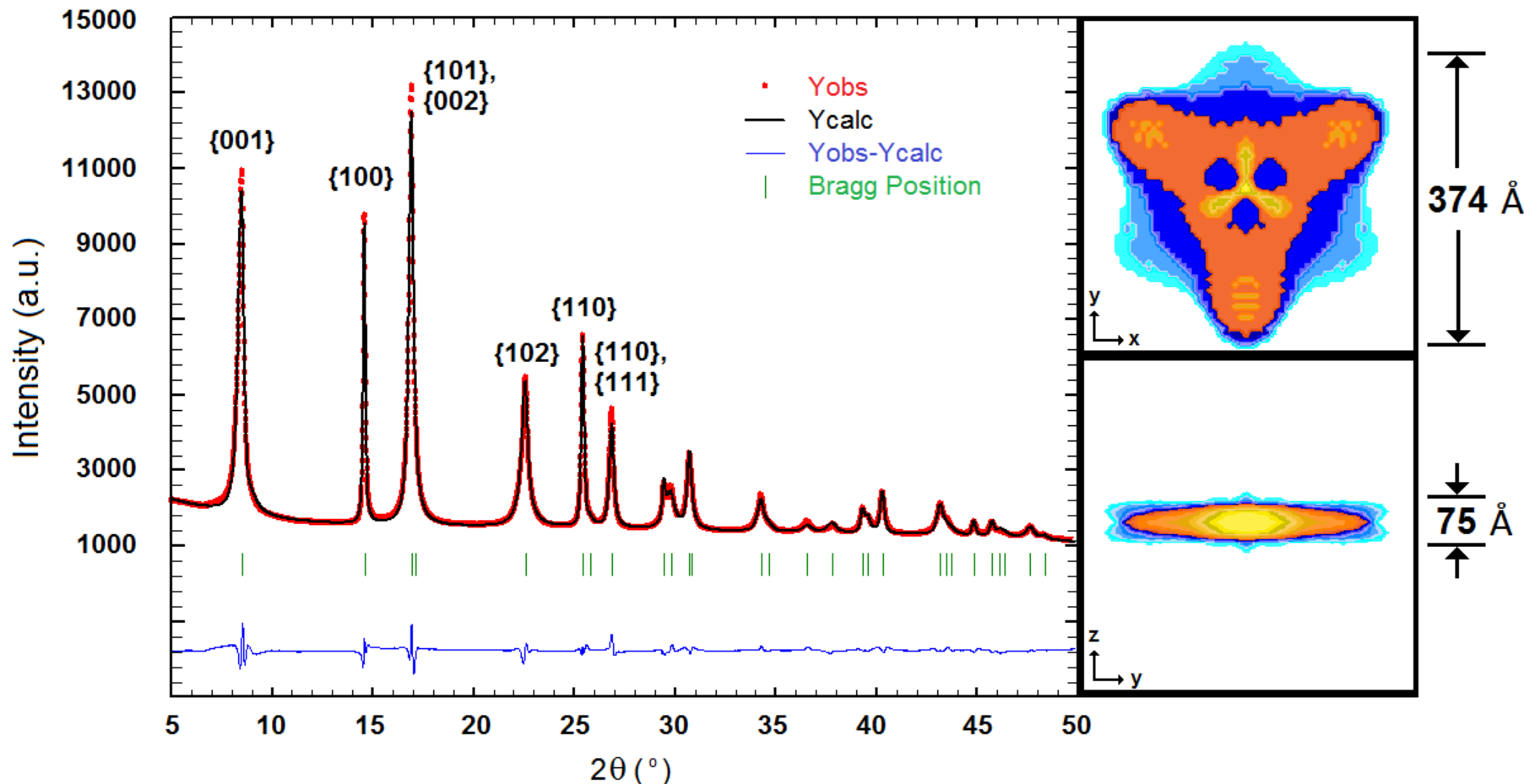


- Powder diffraction reflection profiles can be used to extract grain size and microstrain information.

Round robin raw data from:  
Balzer, D. et. al. J. Appl. Cryst. 37 (2004) 911-924.



# Applications: Crystallite Size and Shape



- $\beta\text{-Ni(OH)}_2$  (theophorastite) crystallizes as hexagonal platelets, the average size of the platelets can be estimated with Rietveld refinement employing an anisotropic size broadening model.



# What is Required for Rietveld Refinement?

- The Rietveld Method is inherently a structure refinement method, **not** a structure solution method.
- Therefore, we need to have a reasonably accurate initial crystal structure model **for each phase** in the sample.
- We also want to have a well aligned, well characterized diffractometer with known instrument parameters.
- To apply the Rietveld method, we need to understand what parameters control our Bragg reflection (1) positions, (2) intensities and (3) peak shapes and breadth.



# Bragg Reflections - Parameters

**Table 8.2** Powder diffraction pattern as a function of various crystal structure, specimen and instrumental parameters.<sup>a</sup>

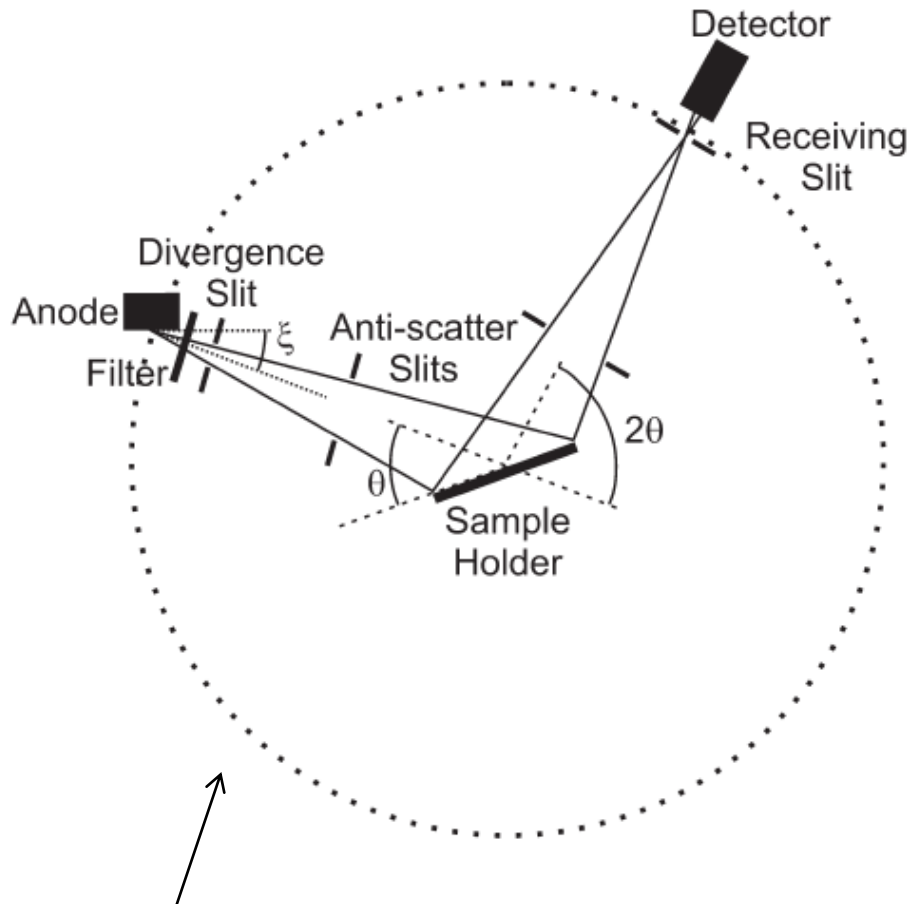
Pattern component	Crystal structure	Specimen property	Instrumental parameter
Peak position	<b>Unit cell parameters:</b> $(a, b, c, \alpha, \beta, \gamma)$	<i>Absorption</i> Porosity  <i>Preferred orientation</i>	<b>Radiation (wavelength)</b> <i>Instrument/sample alignment</i> Axial divergence of the beam
Peak intensity	<b>Atomic parameters</b> $(x, y, z, B, \text{etc.})$	Absorption <i>Porosity</i>	Geometry and configuration <b>Radiation (Lorentz, polarization)</b>
Peak shape	<i>Crystallinity</i> Disorder Defects	<i>Grain size</i> <i>Strain</i> <i>Stress</i>	<b>Radiation (spectral purity)</b> <b>Geometry</b> <b>Beam conditioning</b>

<sup>a</sup> Key parameters are shown in **bold**. Parameters that may have a significant influence are shown in *italic*.

Table taken from: Pecharsky, V. K. & Zavaliy, P. Y., Fundamentals of Powder Diffraction and Structural Characterization of Materials, 2<sup>nd</sup> edition. (Springer: Berlin, 2009).



# Common Powder Diffraction Geometries



Bragg-Brentano  
(reflection)

Debye-Scherrer  
(transmission)

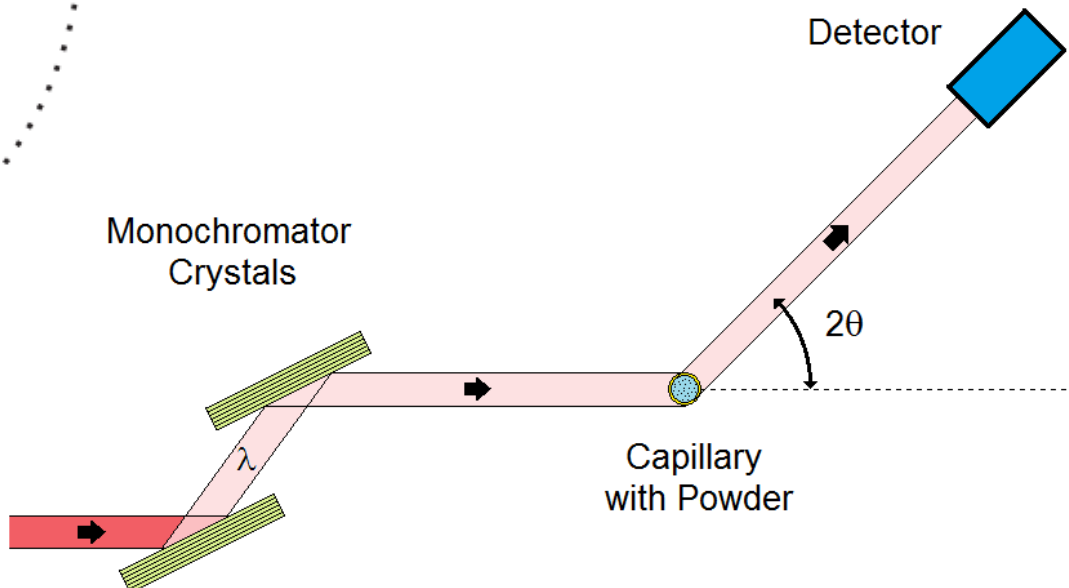


Figure taken from:  
Cockcroft, J.K. & Fitch, A.N. in  
Powder Diffraction, Theory and Practice.  
Edited by R.E. Dinnebier & S.J.L. Billinge.  
(RSC Publishing: Cambridge, 2008)

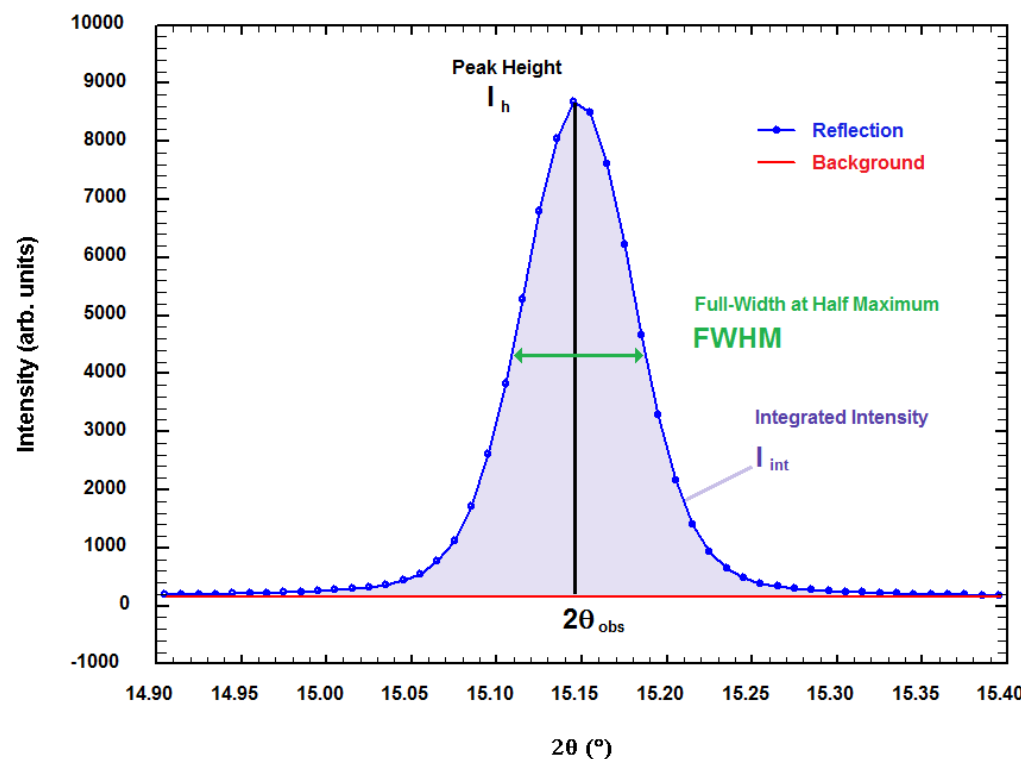


Canadian  
Light  
Source  
Centre canadien  
de rayonnement  
synchrotron

THE BRIGHTEST LIGHT IN CANADA | [lightsource.ca](http://lightsource.ca)

# Bragg Reflection Positions - Parameters

- **Reflection Positions** depend on:
  - X-ray wavelength ( $\lambda$ ),
  - dimensions of the unit cell (lattice parameters  $a, b, c, \alpha, \beta, \gamma$ ),
  - Miller Indices of the diffracting plane in the crystal, &
  - systematic errors which depend on the geometry and sample.

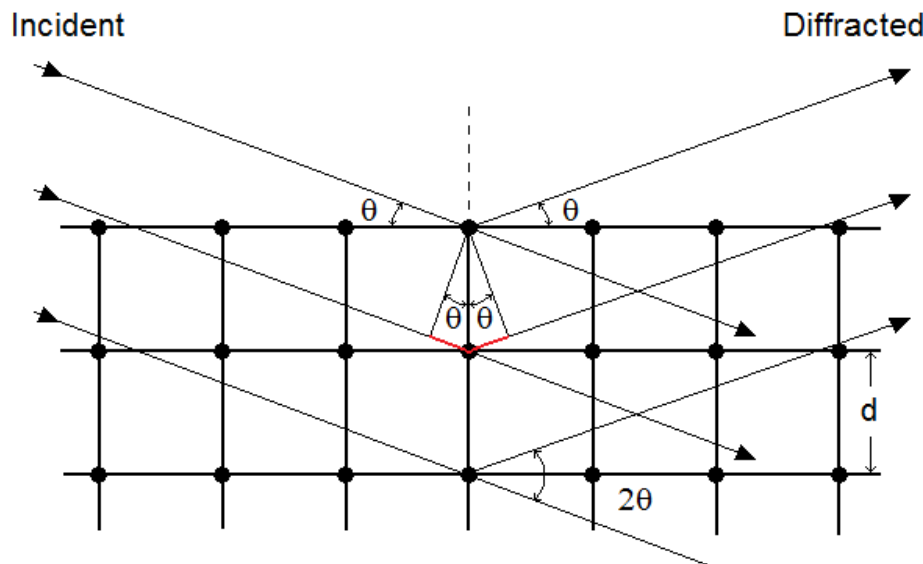


# Reflection Positions - Bragg's Law

- Bragg's law tells us where a diffraction peak will be located (its  $2\theta$  position, in degrees, or  $^\circ$ )
- The peak position depends on the X-ray wavelength ( $\lambda$ ) and the d-spacing between crystal planes ( $d_{hkl}$ ).
- The d-spacing ( $d_{hkl}$ ) depends on the Miller indices of the crystal plane ( $hkl$ ) and lattice parameters of the unit cell.

$$\lambda = 2d_{hkl} \sin \theta$$

$$2\theta_{calc} = 2 \sin^{-1} \left( \frac{\lambda}{2d_{hkl}} \right)$$



# Miller Indices & Interplanar Spacing

- Crystallographic planes are described using **Miller indices ( $hkl$ )**, which are derived from the intercepts of the plane with the crystal axes.

Intercepts, in units of basis vector lengths.

$$s_1, 0, 0 \quad 0, s_2, 0 \quad 0, 0, s_3$$

Invert the intercepts

$$\left( \frac{1}{s_1}, \frac{1}{s_2}, \frac{1}{s_3} \right)$$

Reduce the numbers to the smallest possible integers

$$hkl$$

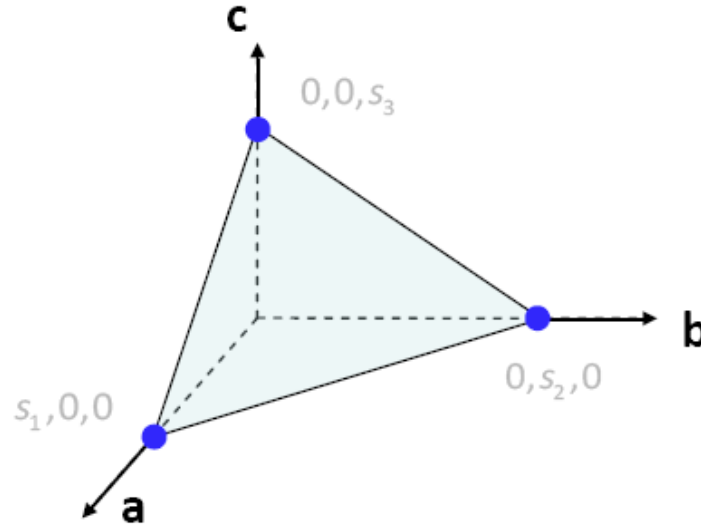


Figure courtesy of Michael Gharghouri.

- The distance between lattice planes (d-spacing or  $d_{hkl}$ ) is given by:

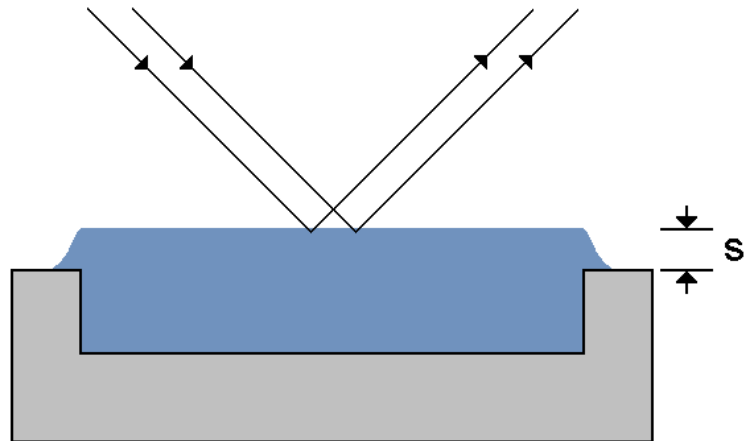
$$d_{hkl} = V [h^2 b^2 c^2 \sin^2 \alpha + k^2 a^2 c^2 \sin^2 \beta + l^2 a^2 b^2 \sin^2 \gamma + 2hlab^2c(\cos \alpha \cos \gamma - \cos \beta)]$$

# Systematic Errors (Bragg-Brentano)

$$2\theta_{obs} = 2\theta_{calc} + \Delta 2\theta$$

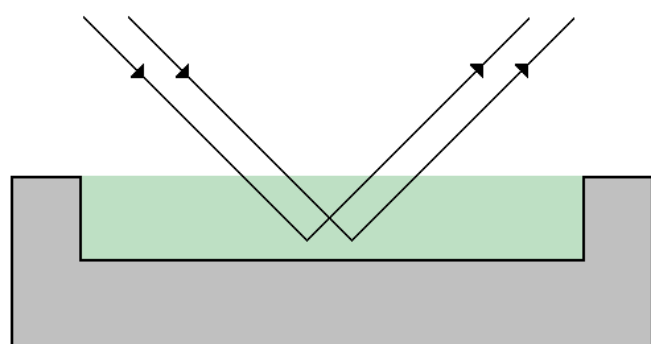
- Sample displacement shift:

$$\Delta 2\theta_{disp} = \frac{-2s}{R} \cos \theta$$



- Sample transparency shift:

$$\Delta 2\theta_{trans} = \frac{1}{2\mu R} \sin 2\theta$$



$R \equiv$  goniometer radius



# Diffraction Pattern Intensity

$$I(2\theta) = I_{bkg} + Lp A_s \sum_p S_p A_p \sum_{hkl} |F_{hkl}|^2 M_{hkl} pV(2\theta - 2\theta_{hkl}) P_{hkl}$$

Diagram illustrating the components of the diffraction pattern intensity equation:

- Background**: Represented by  $I_{bkg}$ .
- Absorption (sample)**: Represented by  $Lp A_s$ .
- Scale Factor (phase  $p$ )**: Represented by  $\sum_p S_p A_p$ .
- Reflection Profile Function**: Represented by  $\sum_{hkl} |F_{hkl}|^2 M_{hkl} pV(2\theta - 2\theta_{hkl}) P_{hkl}$ .
- Structure Factor**: Represented by  $\sum_{hkl} |F_{hkl}|^2 M_{hkl}$ .
- Multiplicity Factor**: Represented by  $pV(2\theta - 2\theta_{hkl}) P_{hkl}$ .
- Texture/Preferred Orientation**: Represented by  $P_{hkl}$ .
- Absorption (phase  $p$ )**: Represented by  $S_p A_p$ .
- Lorentz-polarization correction**: Represented by  $Lp$ .



# Diffraction Pattern Intensity

$$I(2\theta) = I_{bkg} + Lp A_s \sum_p S_p A_p \sum_{hkl} |F_{hkl}|^2 M_{hkl} pV(2\theta - 2\theta_{hkl}) P_{hkl}$$

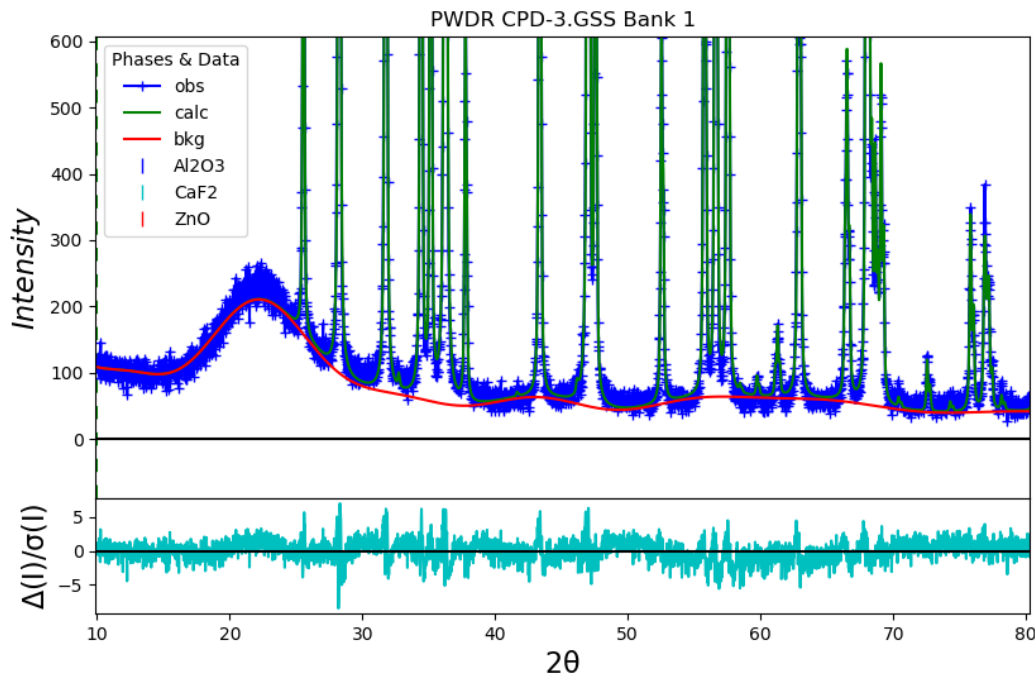
Diagram illustrating the components of the diffraction pattern intensity equation:

- Background** ( $I_{bkg}$ ) is shown in red.
- Absorption (sample)** and **Scale Factor (phase  $p$ )** are combined at the top.
- Reflection Profile Function** is shown on the right.
- Structure Factor** is the product of **Absorption (sample)**, **Scale Factor (phase  $p$ )**, and **Reflection Profile Function**.
- Multiplicity Factor** is the product of **Absorption (phase  $p$ )** and **Texture/Preferred Orientation**.
- Lorentz-polarization correction** is shown on the left.

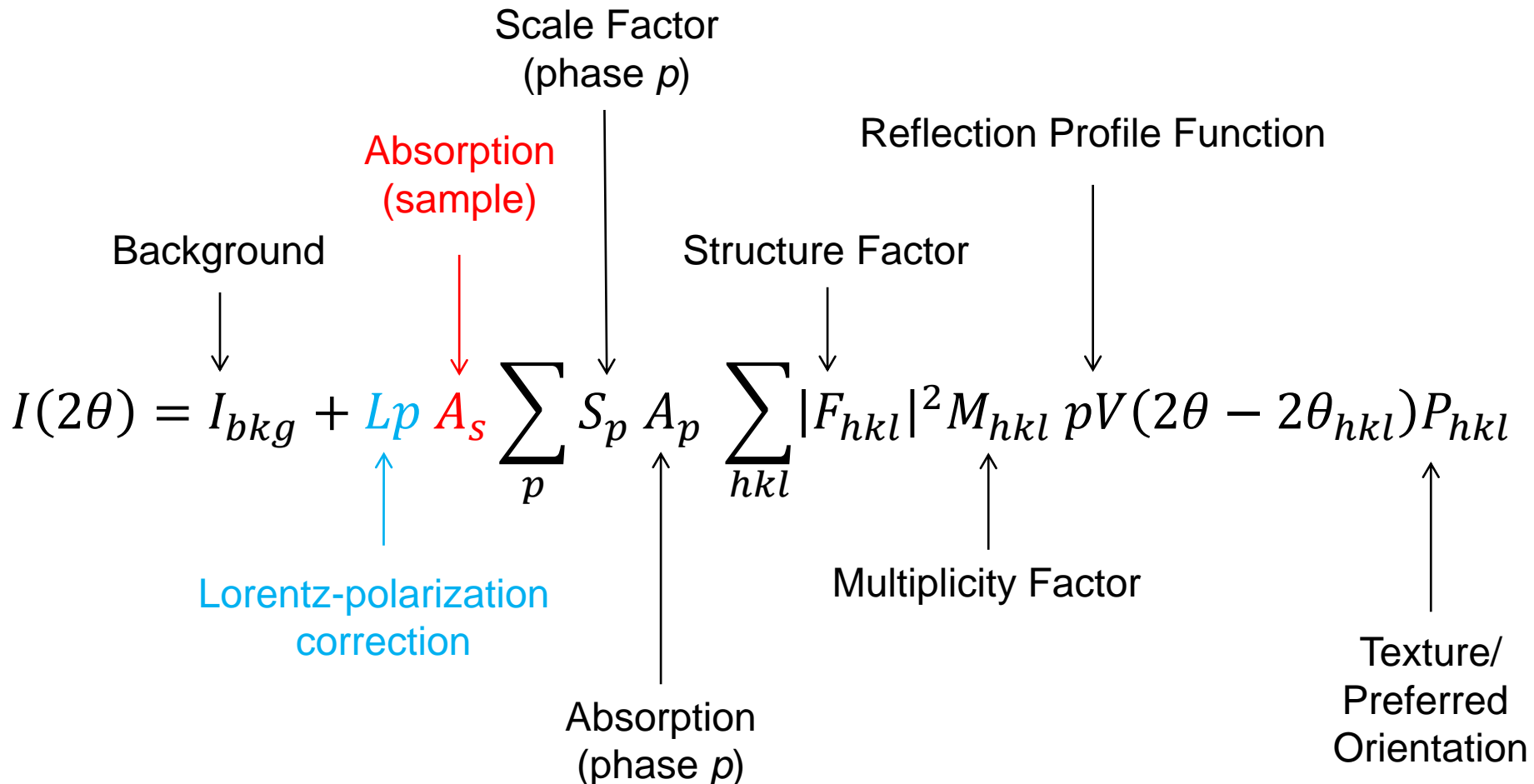


# Background Scattering

- The background of the powder diffraction pattern can be modeled a number of different ways:
  - Empirical functions like the Chebyshev polynomial, cosine Fourier series, power series, etc.
  - Debye function to model amorphous content.
  - Interpolation between fixed or variable background points.



# Diffraction Pattern Intensity



# Lorentz-polarization Factor

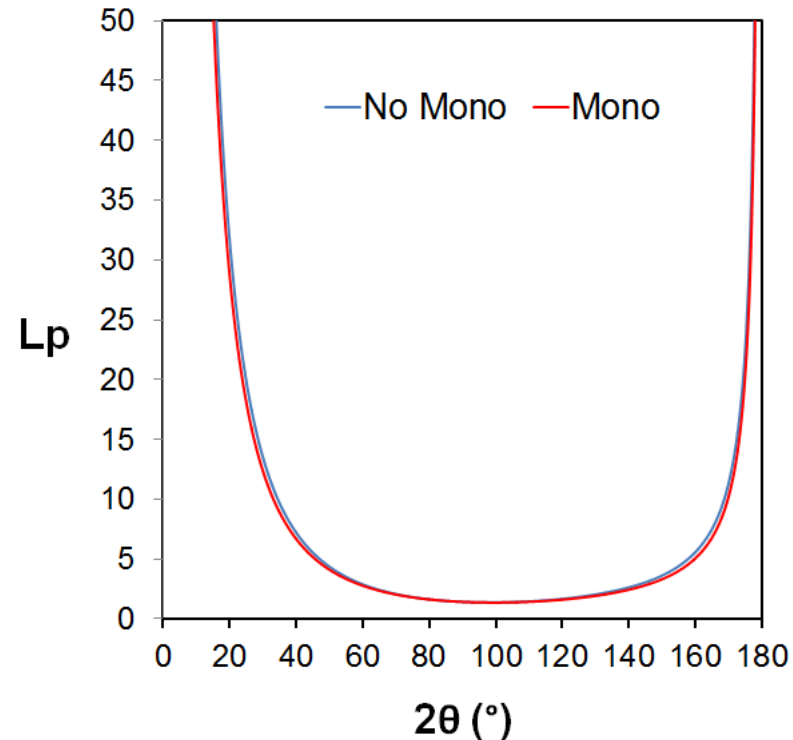
- The Lorentz-polarization ( $L_p$ ) factor combines geometrical effects including the size of the reciprocal lattice points, radii of the Debye rings, and polarization of the incident beam.

$$L_p = \frac{1 - K + K \cdot \cos^2 2\theta \cdot \cos^2 2\theta_M}{\cos \theta \sin^2 \theta}$$

$K \equiv$  fractional polarization

$2\theta_M \equiv$  monochromator angle

For a full derivation of the Lorentz-polarization factor, see:  
Cullity, B.D. Elements of X-ray Diffraction, 2<sup>nd</sup> Ed.  
(Addison-Wesley: Reading, 1978).



# Lorentz-polarization Factor

- The Lorentz-polarization ( $L_p$ ) factor combines geometrical effects including the size of the reciprocal lattice points, radii of the Debye rings, and polarization of the incident beam.

$$L_p = \frac{1 - K + K \cdot \cos^2 2\theta \cdot \cos^2 2\theta_M}{\cos \theta \sin^2 \theta}$$

$K \equiv$  fractional polarization

$2\theta_M \equiv$  monochromator angle

For a full derivation of the Lorentz-polarization factor, see:  
Cullity, B.D. Elements of X-ray Diffraction, 2<sup>nd</sup> Ed.  
(Addison-Wesley: Reading, 1978).

**GSAS2 polarization  
(‘Polariz’ instrument  
parameter):**

Instrument	Polariz.
Unpolarized (no mono)	0.5
Cu K $\alpha$ with Graphite mono	0.7-0.8
Synchrotron	0.9-1.0



# Sample Absorption (Bragg-Brentano)

- The diffracted intensity is reduced by absorption in the specimen according to the transmission coefficient:

$$A = \frac{1}{V} \int e^{-\mu l} dV$$

$\mu \equiv$  linear absorption coefficient  
 $l \equiv$  total path length

- For **Bragg-Brentano** geometry, there are two limiting cases:

- High  $\mu$  (&/or  $t$ )  $\rightarrow A = \frac{\mu}{2}$  (constant, independent of  $2\theta$ )

- Low  $\mu$  (&/or  $t$ )  $\rightarrow A = \frac{1 - e^{\frac{-2\mu t}{\sin \theta}}}{2\mu}$   $t \equiv$  sample thickness



# Sample Absorption (Debye-Scherrer)

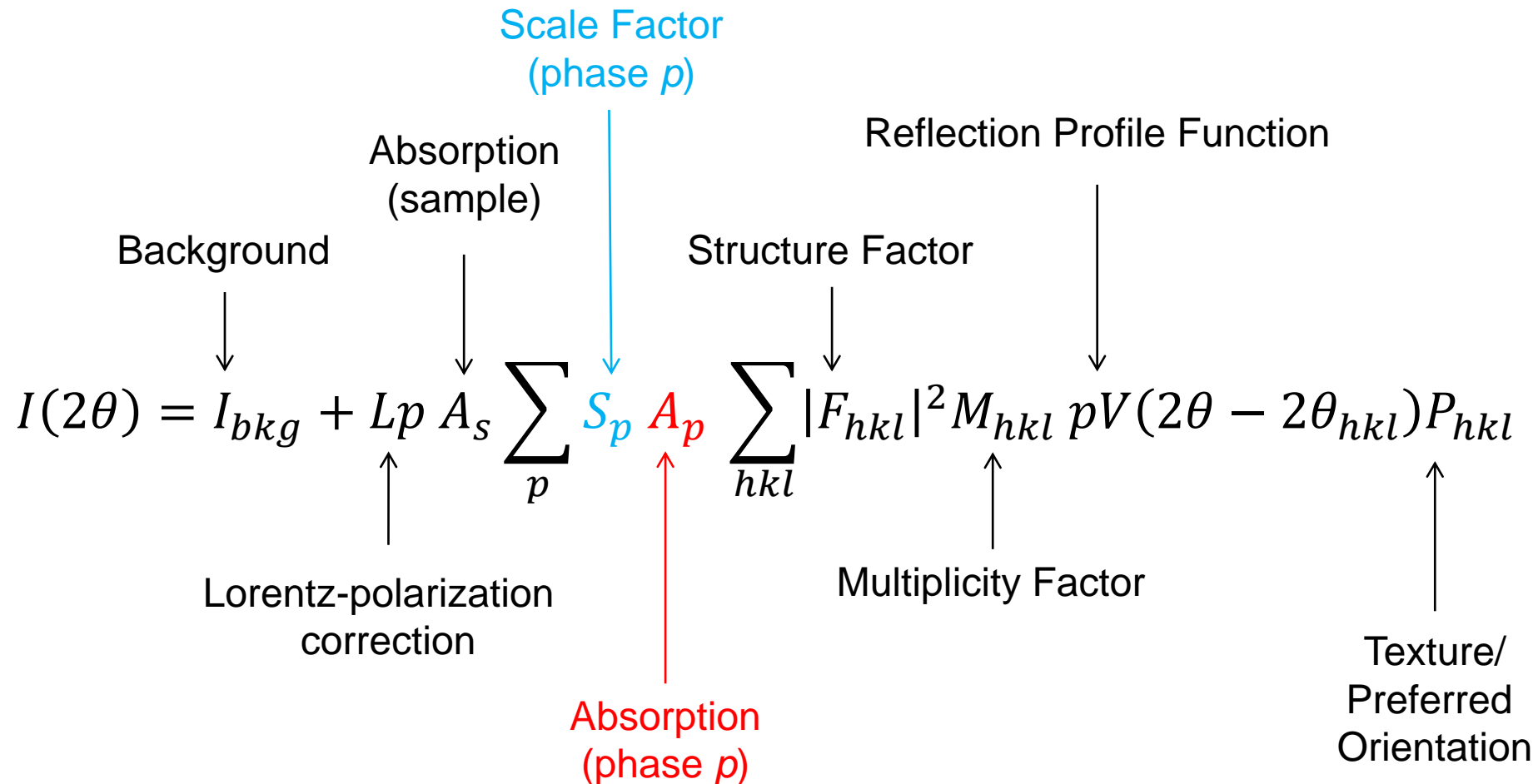
- For **Debye-Scherrer** geometry, the absorption correction depends on  $\mu R$  ( $R$  is the radius of the capillary):

$$A = e^{[-k_0\mu R - k_1(\mu R)^2 - k_2(\mu R)^3 - k_3(\mu R)^4]}$$

- $0 < \mu R < 0.5$  → Low absorption, no correction required.
- $0.5 < \mu R < 1$  → Normal absorption, may need correction for precise thermal parameters.
- $1 < \mu R < 2.5$  → High absorption, correction recommended for analysis.
- $2.5 < \mu R$  → Too high! Re-think your sample preparation.
- APS beamline 11-BM absorption guide & calculator:  
<https://11bm.xray.aps.anl.gov/absorption.html>



# Diffraction Pattern Intensity

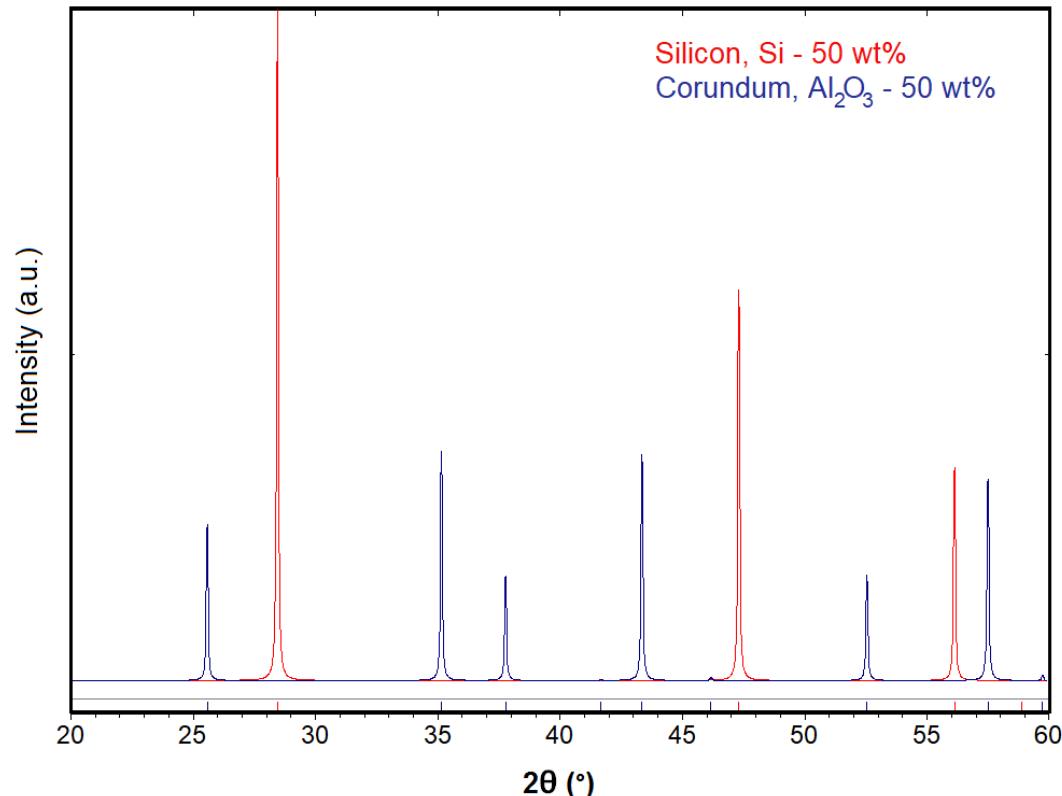


# Scale Factor

- The scale factor ( $S_p$ ) is proportional to the quantity of each phase,  $p$ , present in a mixture, and can be used to estimate the crystalline phase composition,  $W_p$  (weight fraction):

$$W_p = \frac{S_p (ZMV)_p}{\sum_i S_i (ZMV)_i}$$

$Z \equiv$  formula units per unit cell  
 $M \equiv$  molecular mass  
 $V \equiv$  unit cell volume



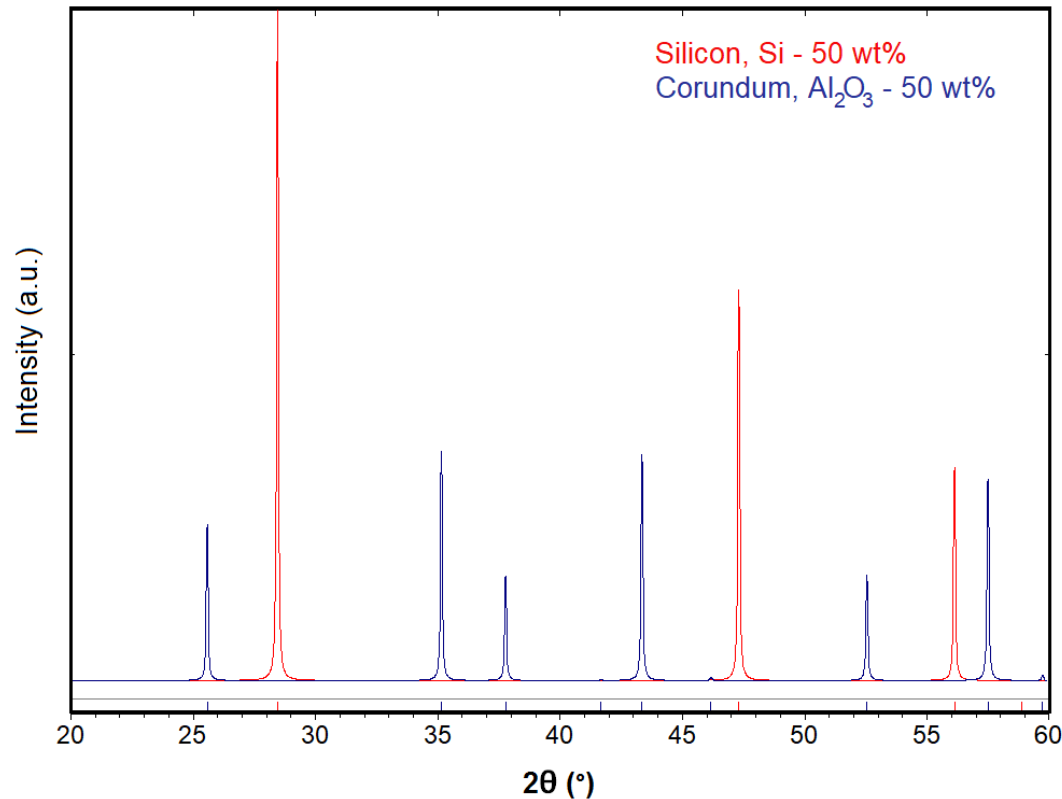
# Scale Factor

- The scale factor ( $S_p$ ) is proportional to the quantity of each phase,  $p$ , present in a mixture, and can be used to estimate the crystalline phase composition,  $W_p$  (weight fraction):

$$W_p = \frac{S_p (ZMV)_p}{\sum_i S_i (ZMV)_i}$$

- The relative intensity of crystalline phases is often compared to Corundum ( $\text{Al}_2\text{O}_3$ ):

For Si:  $I/I_C = \sim 4.5$



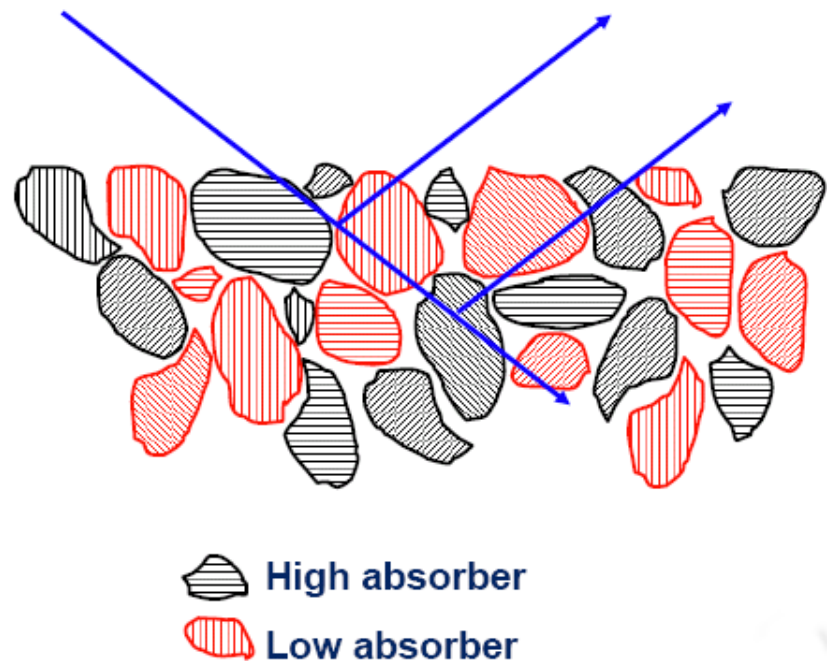
# Absorption – Phase Effects

- For **Bragg-Brentano** geometry, surface roughness and porosity effects can considerably influence reflection intensities:
  - Suortti, P. J. Appl. Cryst. 5 (1972) 383-400.
  - Pitschke, W., Hermann, H., & Mattern, N. Powder Diffraction 8 (1993) 74-83.
  - Pitschke, W., Mattern, N., & Hermann, H. Powder Diffraction 8 (1993) 223-228.
- Results for quantitative phase analysis (QPA) of multiphase mixtures can be strongly influenced by absorption contrast between different phases, called microabsorption:
  - Brindley, G.W. Philosophical Magazine 3 (1945) 347-369.
  - Scarlett, N. V. Y., et al. J. Appl. Cryst. 35 (2002) 383-400.
  - Scarlett, N. V. Y. & Madsen, I.C. Powder Diffraction 33 (2018) 26-37.



# Absorption – Phase Effects

- **Microabsorption**, or contrast in a mixture of high and low absorbing phases, is often the biggest obstacle encountered for accurate quantitative phase analysis (QPA).
- High absorbing phases have diffraction restricted to the particle surface and tend to be underestimated.
- Low absorbing phases diffract from the entire volume and tend to be overestimated.



Brindley, G.W. Philosophical Magazine 3 (1945) 347-369.  
Scarlett, N. V. Y., et al. J. Appl. Cryst. 35 (2002) 383-400.  
Scarlett, N. V. Y. & Madsen, I.C. Powder Diffraction 33 (2018) 26-37.

Figure courtesy of Pamela Whitfield.



Canadian  
Light  
Source

Centre canadien  
de rayonnement  
synchrotron

THE BRIGHTEST LIGHT IN CANADA | [lightsource.ca](http://lightsource.ca)

# Mitigating Microabsorption

- Microabsorption can be minimized by:
  - Making sure your sample has been very well ground or micronized to obtain the smallest possible particle sizes (the degree to which microabsorption is an issue is proportional to the product of the linear absorption coefficient and particle size,  $\mu D$ ).
  - Using higher energy radiation (synchrotron, if available); absorption decreases with increasing X-ray energy.
  - Using neutrons (if available); not always easy to access, but the gold standard solution for microabsorption.
- Brindley devised a correction based on knowing  $\mu D$  (i.e. average particle sizes) for each phase which can work in ideal cases, but is typically impractical.

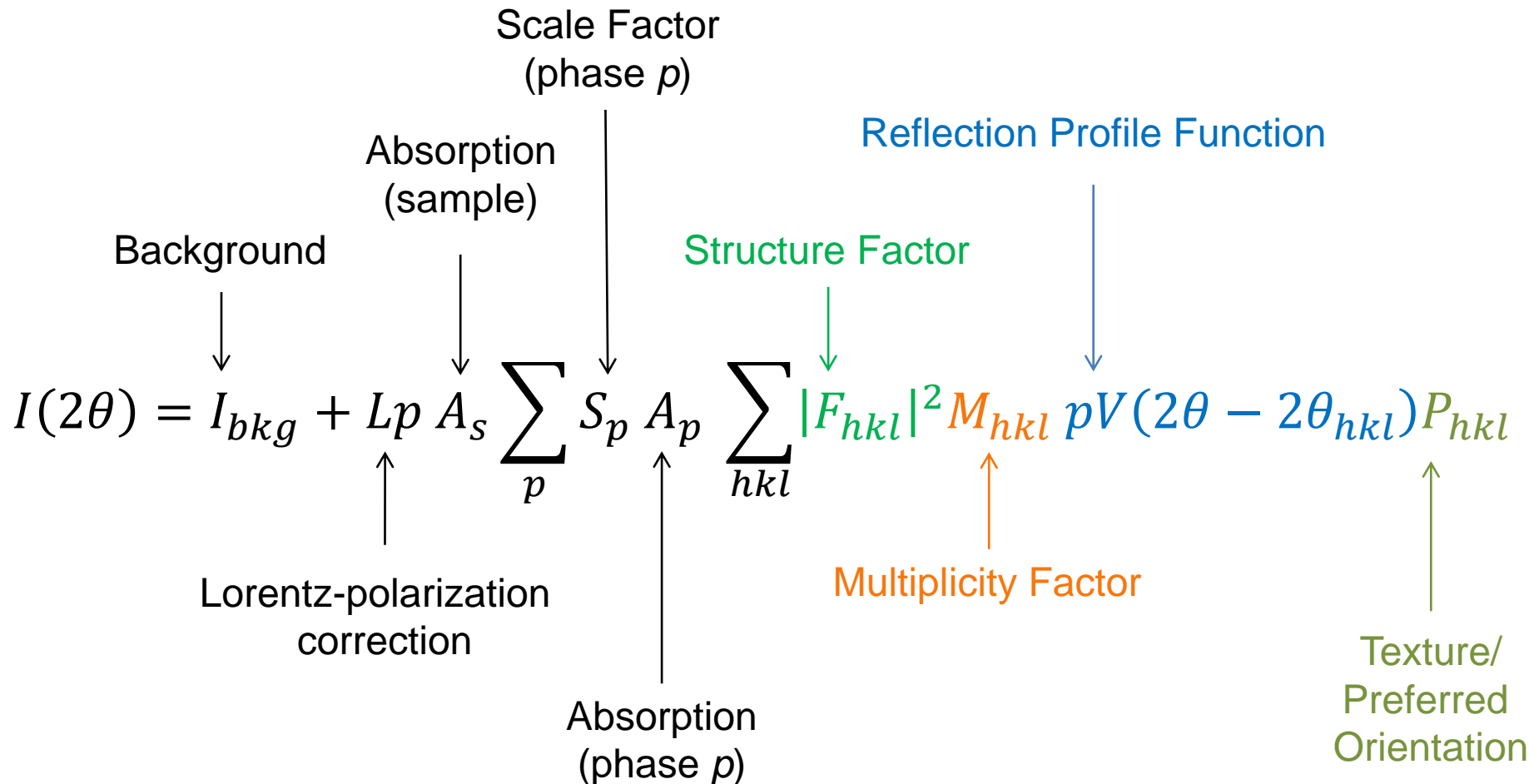
Brindley, G.W. Philosophical Magazine 3 (1945) 347-369.

Scarlett, N. V. Y., et al. J. Appl. Cryst. 35 (2002) 383-400.

Scarlett, N. V. Y. & Madsen, I.C. Powder Diffraction 33 (2018) 26-37.



# Diffraction Pattern Intensity



# Structure Factor

- The structure factor relates the atomic positions, atomic species (via the atomic scattering factor) and thermal displacement (via the thermal factor) to the intensity of individual  $hkl$  reflections:

Displacement (Debye-Waller) Factor

$$F_{hkl} = \sum_j N_j f_j e^{-B_j \left(\frac{\sin \theta}{\lambda}\right)^2} e^{2\pi i(hx_j + ky_j + lz_j)}$$

↑  
Site Occupancy

↑  
Atomic Scattering Factor

↑  
Fractional atomic coordinates

$$F_{hkl} = \frac{\text{amplitude scattered by the atoms in the unit cell}}{\text{amplitude scattered by a single electron}}$$



# Atomic Scattering Factor

$$f = \frac{\text{amplitude scattered by an atom}}{\text{amplitude scattered by a single electron}}$$

- Light elements scatter X-rays relatively poorly.
- The intensities of X-ray diffraction peaks decrease rapidly with increasing diffraction angle ( $2\theta$ ).

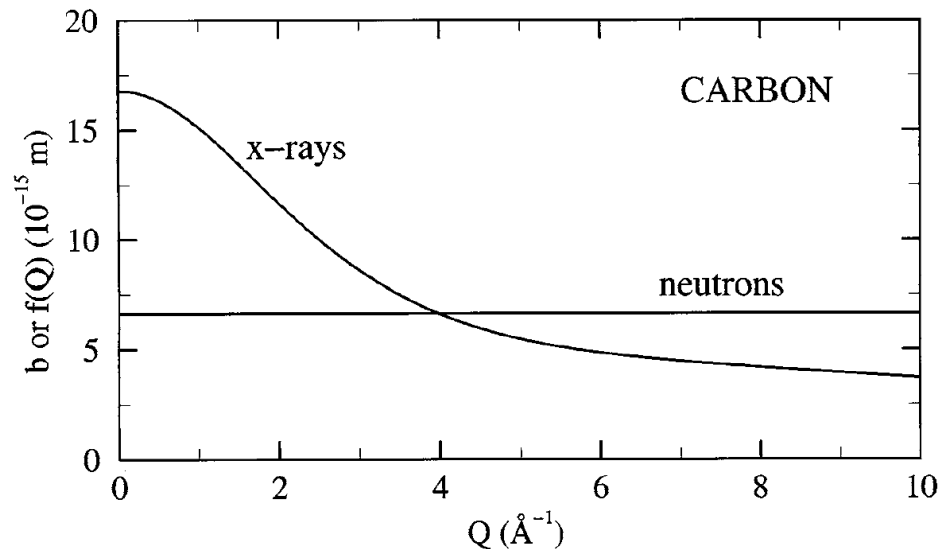


Figure taken from: Copley, J.R.D. *Natl. Inst. Stand. Technol. Spe. Pub.* 960-2 (2001).

# Comparison of Atomic Form Factors

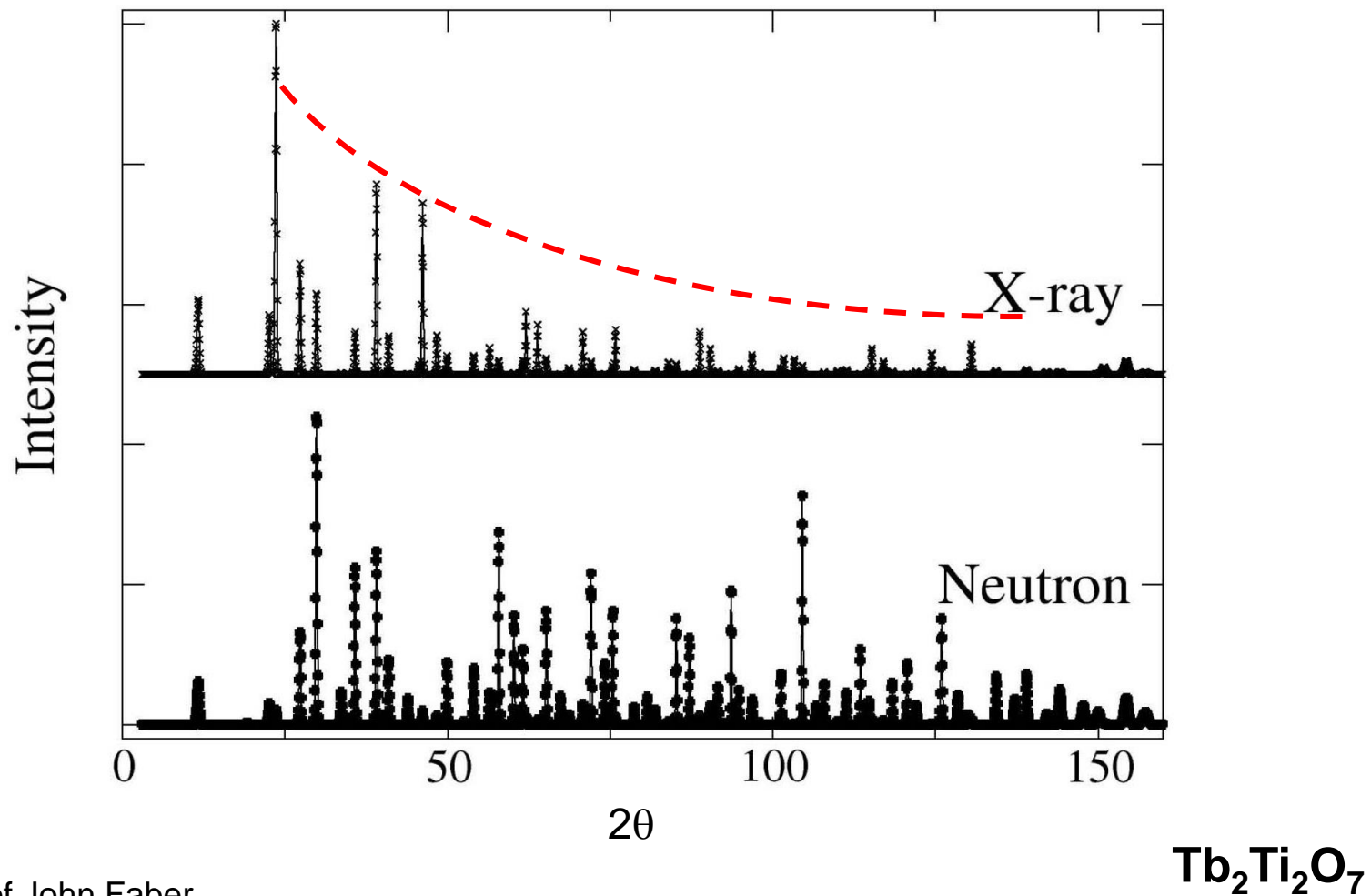


Figure courtesy of John Faber



Canadian  
Light  
Source

Centre canadien  
de rayonnement  
synchrotron

THE BRIGHTEST LIGHT IN CANADA | [lightsource.ca](http://lightsource.ca)

# Comparison of Atomic Form Factors

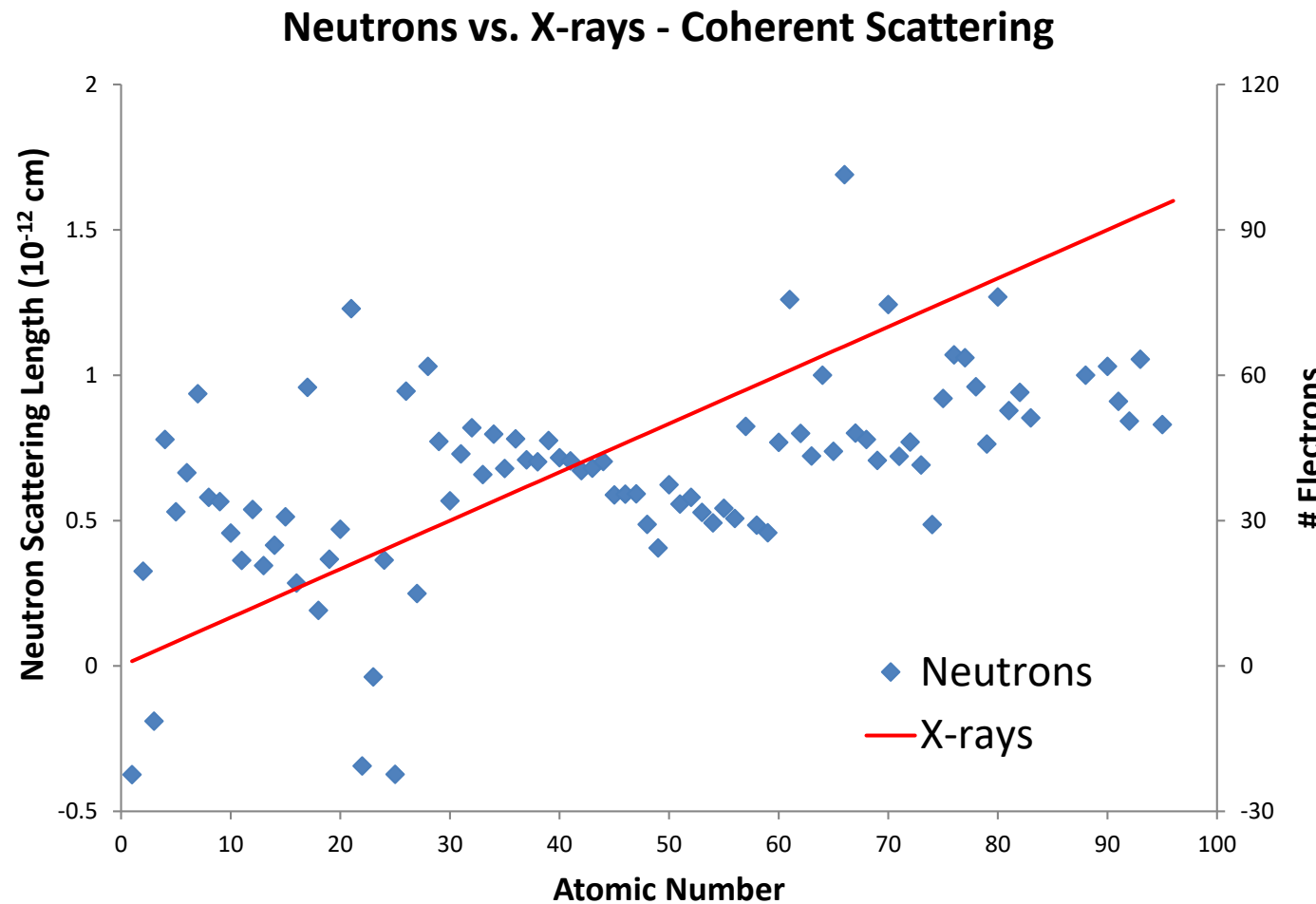


Figure courtesy of John Faber



Canadian  
Light  
Source

Centre canadien  
de rayonnement  
synchrotron

THE BRIGHTEST LIGHT IN CANADA | [lightsource.ca](http://lightsource.ca)

# Atomic Scattering Factor

$$f = \frac{\text{amplitude scattered by an atom}}{\text{amplitude scattered by a single electron}}$$

- Light elements scatter X-rays relatively poorly.
- The intensities of X-ray diffraction peaks decrease rapidly with increasing diffraction angle ( $2\theta$ ).

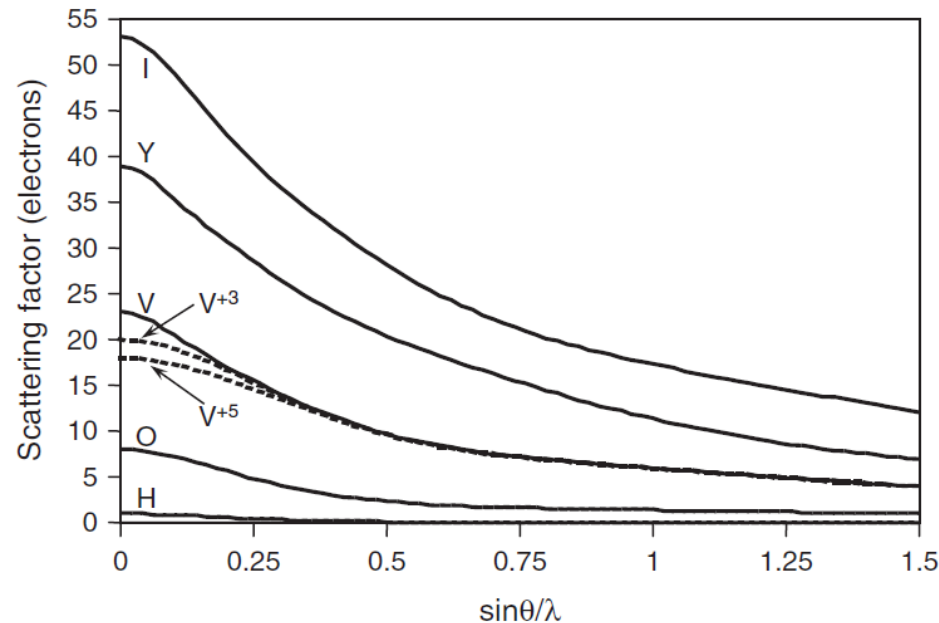


Figure taken from: Pecharsky, V. K. & Zavalij, P. Y., Fundamentals of Powder Diffraction and Structural Characterization of Materials, 2<sup>nd</sup> edition. (Springer: Berlin, 2009).

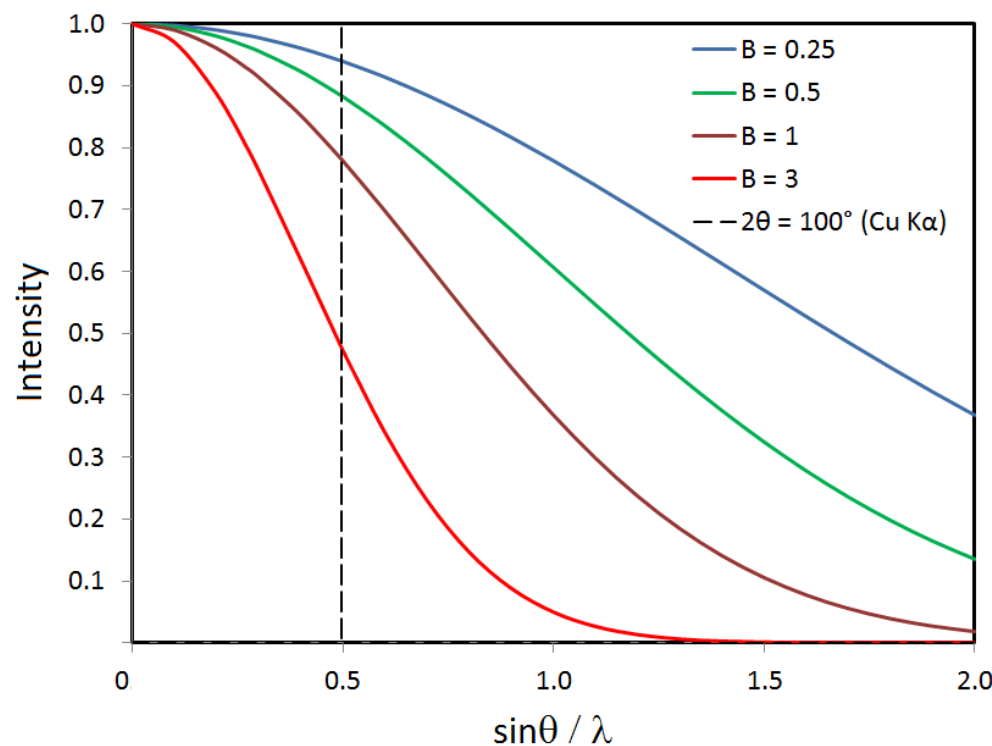
# Displacement Parameter

- The displacement parameter reflects thermal and vibrational motion in the atoms from their equilibrium positions which attenuates the reflection intensities:

$$e^{-B_j \left( \frac{\sin \theta}{\lambda} \right)^2}$$

$$B_j = 8\pi^2 u_j^2 = 8\pi^2 U_j$$

- $B_j$  is called the Debye-Waller factor and  $U_j$  is the root mean squared thermal displacement of the atom.



# Reflection Multiplicity

48 - {hkl}

- The multiplicity reflects the number of equivalent planes (or equivalent grain orientations to diffract) belonging to a set of  $hkl$  indices.

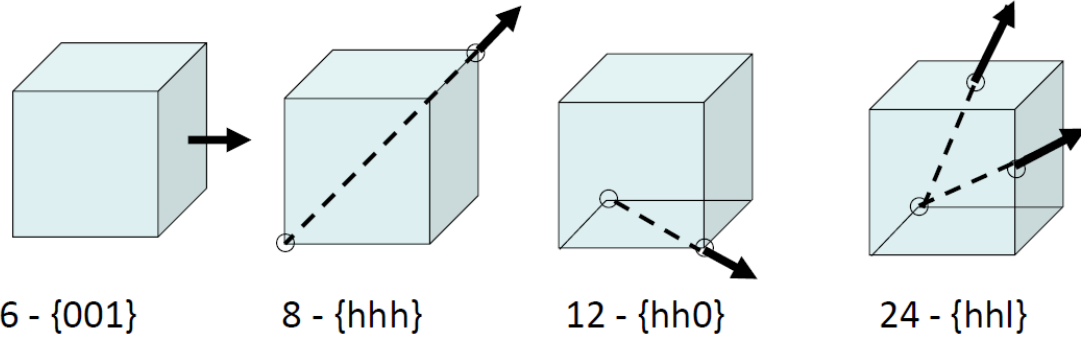


Figure courtesy of Michael Gharghouri.

System	$hkl$	$hhl$	$hh0$	$0kk$	$hhh$	$hk0$	$hol$	$0kl$	$h00$	$k00$	$00l$
Cubic	48*	24	12	12	8	24*	24*	24*	6	6	6
Tetragonal	16*	8	4	8	8	8*	8	8	4	4	2
Hexagonal	24*	12*	6	12	12	12*	12*	12*	6	6	2
Orthorhombic	8	8	8	8	8	4	4	4	2	2	2
Monoclinic	4	4	4	4	4	4	2	4	2	2	2
Triclinic	2	2	2	2	2	2	2	2	2	2	2

Asterisk (\*) indicates non-equivalence of planes may reduce this number by half in some circumstances.



# Reflection Profile Functions

- X-ray diffraction reflections tend to be mixtures (mixing parameter  $\eta$ ) of Gaussian (G) and Lorentzian (L) distributions which are typically combined in what is called a pseudo-Voigt (pV) function:

$$pV(2\theta) = \eta L(2\theta) + (1 - \eta)G(2\theta)$$

$$G(2\theta) = \left[ \frac{2}{\Gamma_G} \right] \sqrt{\frac{\ln 2}{\pi}} e^{\frac{-4 \ln 2 (2\theta - 2\theta_{hkl})^2}{\Gamma_G^2}}$$

$$L(2\theta) = \frac{2}{\pi \Gamma_L} \frac{4(2\theta - 2\theta_{hkl})^2}{1 + \frac{4(2\theta - 2\theta_{hkl})^2}{\Gamma_L^2}}$$

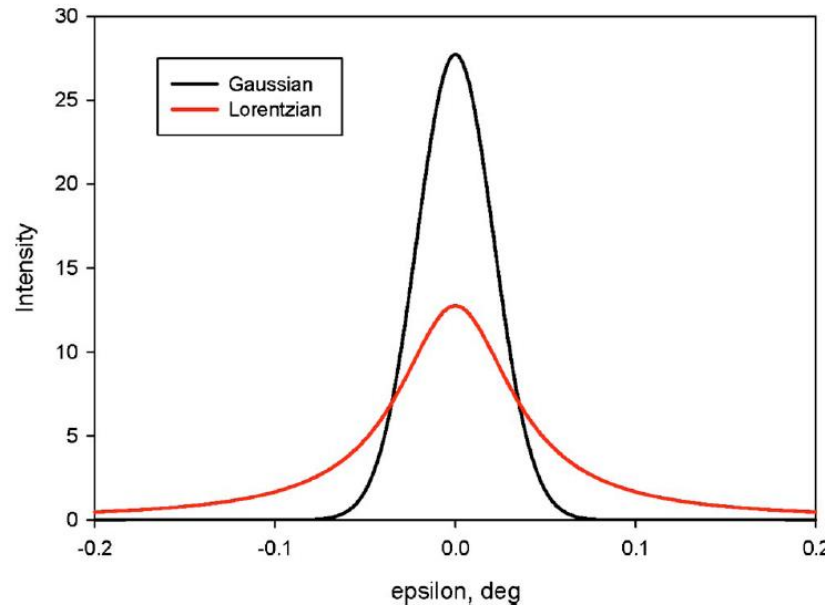


Figure taken from: Kaduk, J.A. & Reid, J. Powder Diffraction 26 (2011) 88-93.



# Reflection Profile Functions

- A parameterization of the pseudo-Voigt called the Thompson-Cox-Hastings pseudo-Voigt (TCH-pV) model (Thompson, P. et al. *J. Appl. Cryst.* 20 (1987) 79-83) is commonly used in Rietveld software because it makes it relatively easy to relate the full width at half maximum (FWHM or  $\Gamma$ ) parameters to instrument resolution and specimen broadening effects:

$$\Gamma_G^2 = \textcolor{blue}{U} \tan^2 \theta + V \tan \theta + W + \frac{\textcolor{red}{P}}{\cos^2 \theta}$$

‘Mostly’  
instrument  
broadening

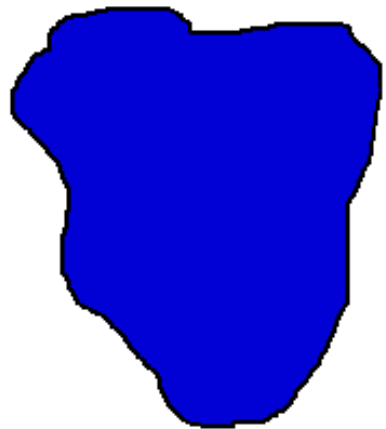
$$\Gamma_L = \frac{\textcolor{red}{X}}{\cos \theta} + \textcolor{blue}{Y} \tan \theta$$

‘Mostly’ sample  
broadening

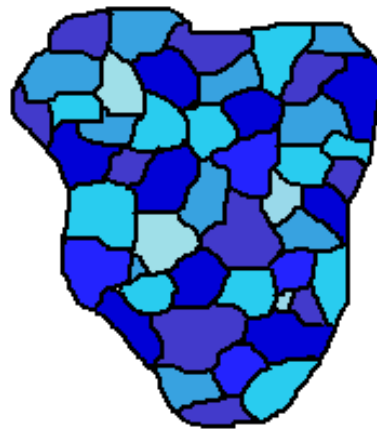
- The  $1/\cos \theta$  coefficients ( $P, X$ ) tend to correlate to size broadening, while the  $\tan \theta$  coefficients ( $U, Y$ ) tend to correlate to strain broadening.



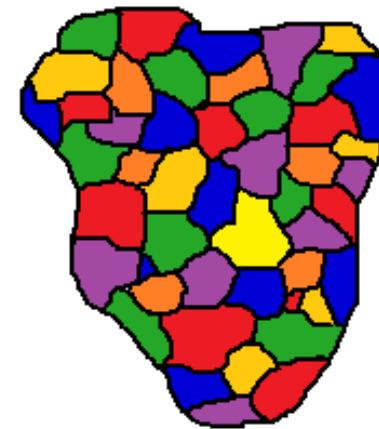
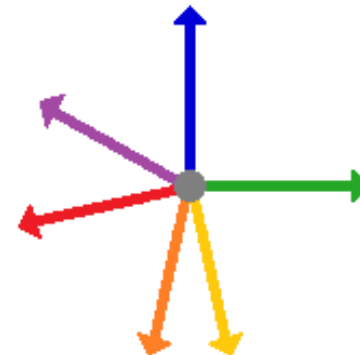
# Preferred Orientation/Texture



**Single  
Crystal**

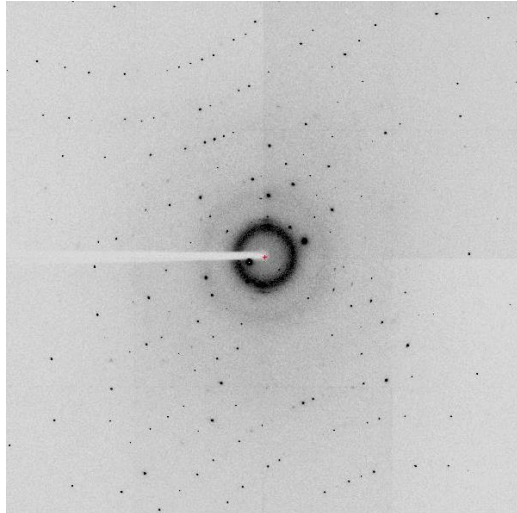


**Textured  
Polycrystal**

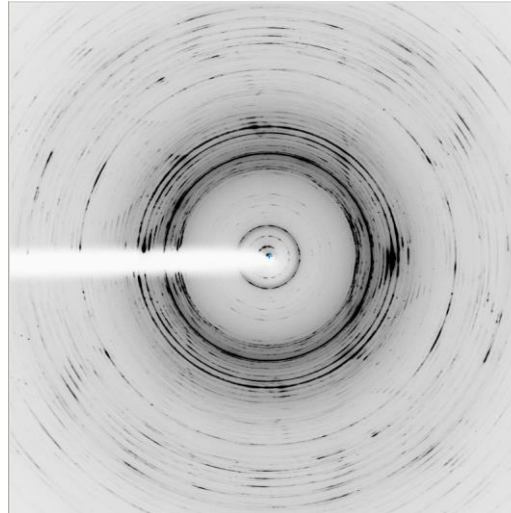


**Random  
Powder**

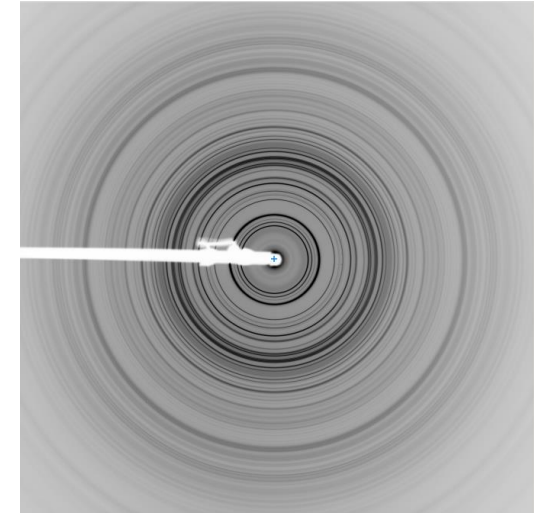
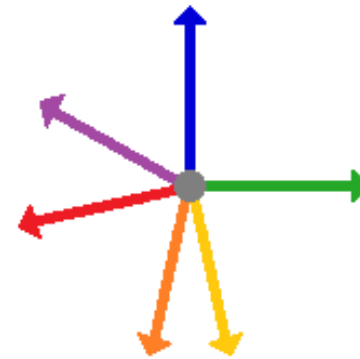
# Preferred Orientation/Texture



**Single  
Crystal**



**Textured  
Polycrystal**



**Random  
Powder**

Textured pattern courtesy of Saeed Ghazani and Alejandro Marangoni.



# Preferred Orientation/Texture

- Straightforward cases of preferred orientation, typically platelet or needle morphologies, can be adequately refined using the March-Dollase model:
  - Dollase, W. A. J. Appl. Cryst. 19 (1986) 267-272.
- More complicated cases require a general orientation distribution function (ODF) approach using spherical harmonics:
  - Von Dreele, R. B. J. Appl. Cryst. 30 (1997) 517-525.
  - Bunge, H. J., Textures and Microstructure 29 (1997) 1-26.



# Diffraction Pattern Intensity

$$I(2\theta) = I_{bkg} + Lp A_s \sum_p S_p A_p \sum_{hkl} |F_{hkl}|^2 M_{hkl} pV(2\theta - 2\theta_{hkl}) P_{hkl}$$

Diagram illustrating the components of the diffraction pattern intensity equation:

- Background**: Represented by  $I_{bkg}$ .
- Absorption (sample)**: Represented by  $Lp A_s$ .
- Scale Factor (phase  $p$ )**: Represented by  $\sum_p S_p A_p$ .
- Reflection Profile Function**: Represented by  $\sum_{hkl} |F_{hkl}|^2 M_{hkl} pV(2\theta - 2\theta_{hkl}) P_{hkl}$ .
- Structure Factor**: Represented by  $\sum_{hkl} |F_{hkl}|^2 M_{hkl}$ .
- Multiplicity Factor**: Represented by  $pV(2\theta - 2\theta_{hkl}) P_{hkl}$ .
- Texture/Preferred Orientation**: Represented by  $P_{hkl}$ .
- Absorption (phase  $p$ )**: Represented by  $S_p A_p$ .
- Lorentz-polarization correction**: Represented by  $Lp$ .



# Summary

- Powder diffraction is a comprehensive technique for studying crystalline materials with crystal sizes ranging from microns ( $10^{-6}$  m) to nanometers ( $10^{-9}$  m), across many scientific fields (mineralogy, advanced materials, pharmaceutical science, catalysis, forensics, etc.).
- The Rietveld method is not a structure solution method, it's a refinement method. A reasonable starting model is needed for each phase in your sample.
- To make the most of Rietveld refinement, you need a basic understanding of the physical underpinnings of the powder diffraction pattern.



# Acknowledgements

- A sincere thank you to Jim Kaduk, John Faber, Michael Gharghouri, Pam Whitfield, Denis Spasyuk, Saeed Ghazani & Alejandro Marangoni for the liberal use of their figures, ideas and knowledge.



# Further Reading

- Pecharsky, V.K. & Zavalij, P.Y. Fundamentals of Powder Diffraction and Structural Characterization of Materials, 2<sup>nd</sup> Ed.  
Springer: New York, 2009.
- Dinnebier, R.E. & Billinge, S.J.L., ed. Powder Diffraction, Theory and Practice.  
RSC: Cambridge, 2009.
- Young, R.A., ed. The Rietveld Method.  
Oxford: New York, 1993.
- Warren, B.E. X-ray Diffraction.  
Dover: New York, 1990.
- Klug, H.P. & Alexander, L.E. X-ray Diffraction Procedures for Polycrystalline and Amorphous Materials, 2<sup>nd</sup> Ed.  
Wiley: New York: 1974.

